

EXPERIMENTAL AND COMPUTER MODELING TO CHARACTERIZE THE
PERFORMANCE OF CRICKET BATS

By

HARSIMRANJEET SINGH

A thesis submitted in partial fulfillment of
the requirements for the degree of

MASTER OF SCIENCE IN MECHANICAL ENGINEERING

WASHINGTON STATE UNIVERSITY
School of Mechanical and Materials Engineering
December 2008

To the Faculty of Washington State University:

The members of the Committee appointed to examine the thesis of Harsimranjeet Singh find it satisfactory and recommend that it be accepted.

Chair

ACKNOWLEDGEMENT

First, I would like to thank my parents and my brother for their support and guidance throughout my life. Without them, getting this far in life would not be possible.

Secondly, I would like to special thank Dr. Lloyd V. Smith for his advice, careful guidance, instruction and immeasurable patience throughout this project. I am thankful for the opportunity to have worked on a unique project that helped me to understand and improve as a sportsman in this game. I would like to thank the other committee members Dr. Sankar Jayaram and Dr. Uma Jayaram for their support and help to focus on my work to complete this project. I appreciate their feedback and willingness to help with my research. I am thankful especially to Dr. Sankar Jayaram for guiding and helping me to buy equipment for this project.

This project would not be possible without the staff in the Mechanical Engineering department. I am also thankful to Henry, and Giac for their help and answering all my questions I have concerning the project I was performing. I would like to thank my coworkers, Rossana Anderson, Zac Kramer, Amanada Kramer, Ryan Smith, Nick Smith and Warren Faber, I enjoyed working with you all. In addition, thank you to Gayle Landeen, Robert Ames, and Mary Simonsen in the MME office for putting up with me.

Outside of school, I would like to thank my friends, Harminder Pooni, Gurjot Gill, Karamveer Singh and all the cricket team for their enthusiasm and encouragement. I would especially thank to Harminder Pooni for her charming nature and always believing that I will make it.

EXPERIMENTAL AND COMPUTER MODELING TO CHARACTERIZE THE
PERFORMANCE OF CRICKET BATS

Abstract

by Harsimranjeet Singh, M.S.
Washington State University
December 2008

Chair: Lloyd V. Smith

The performance of cricket bats depend upon the properties of cricket balls, bat swing speed, and the nature of the wood. An experimental test apparatus was developed to measure the performance of cricket bats and balls representative of play conditions. Experiments were carried out to measure the coefficient of restitution (COR) and hardness of the cricket balls. The ball COR and hardness of seam impacts was slightly higher than face impacts (~1%). Thus bat performance and durability should be insensitive to ball orientation.

A bat performance measure was derived in terms of an ideal batted-ball speed (BBS) based on play conditions. The average performance of four bats was nearly unchanged from knock-in (a common treatment to new cricket bats), (knock-in decreased performance <0.1%). Wood species also had a small effect on the bat performance. A composite skin, applied to the back of some bats, was observed to increase performance measurably, but still by a relatively small amount (1.4%). While different treatments of cricket bats had a measurable effect on performance, they were smaller than the 10% difference observed between solid wood and hollow baseball and softball bats.

A dynamic finite element model was employed to simulate the bat-ball impact. The ball was modeled as a linear viscoelastic material, which provided for energy loss during impact. The ball model was tuned to agree with the measured COR and impact force. The model found good agreement with experimental bat performance data for all impact conditions considered. A model of a composite skin applied to the back of the bat increased performance comparable to that found experimentally. Weight was added to the model at different points on the cricket bat to study the effect of inertia on bat performance. Increasing the moment of inertia by 15% increased the batted-ball speed by 1%.

TABLE OF CONTENTS

	Page
ACKNOWLEDGEMENTS	iii
ABSTRACT	iv
TABLE OF CONTENTS	vi
LIST OF TABLES	ix
LIST OF FIGURES	x
CHAPTER ONE	
INTRODUCTION	1
REFERENCES	8
CHAPTER TWO	
LITERATURE REVIEW	9
2.1 Ball Response	9
2.1.1 Coefficient of Restitution	9
2.1.1.a Defination and History	9
2.1.1.b COR Models	1
2.1.2 Dynamic Ball Hardness	13
2.1.3 Construction of Cricket Ball	15
2.1.4 Ball Model	16
2.2 Bat Response	18
2.2.1 Bat Performance metrics	18
2.2.2 Field Conditions	19
2.2.3 Bat Composition	21
2.2.4 Bat Numerical Model	22
2.2.5 Bat Constraint	23
2.3 Summary	24
REFERENCES	26

CHAPTER THREE

BALL TESTING.....	30
3.1 Introduction.....	30
3.2 Ball Testing Apparatus.....	31
3.3 Test Speed.....	34
3.4 Dynamic Properties.....	37
3.5 COR and Dynamic Stiffness Results	38
3.6 Rate Dependence.....	41
3.7 Static Compression.....	45
3.8 Summary.....	48
REFERENCES.....	50

CHAPTER FOUR

BAT TESTING.....	51
4.1 Introduction.....	51
4.2 Experimental Apparatus Setup.....	53
4.2.1 MOI Apparatus.....	53
4.2.2 Bat Testing Equipment.....	55
4.3 Bat Performance Metric.....	56
4.4 Test Results.....	60
4.4.1 Knock-in/Oiled.....	60
4.4.2 Material Comparison	62
4.5 Summary.....	66
REFERENCES.....	67

CHAPTER FIVE

NUMERICAL MODEL

5.1 Introduction.....	69
5.2 Ball Model.....	69
5.2.1 Numerical Analysis Background.....	69
5.2.2 Model Tuning with Experimental Results.....	75

5.2.3	Rate Dependence.....	80
5.3	Bat Model.....	82
5.3.1	Numerical Model.....	82
5.3.2	Bat Models and Materials.....	83
5.3.3	Modeling the Bat- Ball Impact.....	86
5.4	Experimental Comparison.....	87
5.4.1	Weight Study.....	89
5.4.2	Composite Skin.....	90
5.5	SUMMARY.....	91
	REFERENCES.....	93

CHAPTER SIX

	SUMMARY AND FUTURE WORK.....	94
6.1	Review.....	94
6.2	Ball Testing.....	94
6.3	Bat Testing.....	94
6.4	Numeric Model.....	95
6.5	Future Work.....	95

APPENDIX ONE

	Detailed information used for cricket bat model with composite skin.....	97
--	--	----

APPENDIX TWO

	Detailed information used for cricket bat model in weight study.....	101
--	--	-----

APPENDIX THREE

	Detailed information used for cricket ball model.....	104
--	---	-----

LIST OF TABLES

Table 4.1: Properties of different cricket bats.....	54
Table 5.1: Viscoelastic properties of cricket ball used in following figures	74
Table 5.2: Viscoelastic parameter values of softball and baseball	77
Table 5.3: Values of viscoelastic properties used in the study for bat-tuned model	82
Table 5.4: Values of viscoelastic properties used in the study for bat-tuned model	84
Table 5.5: Elastic properties of cricket bat (coordinate system as in Fig. 5.14 and 5.15).....	85
Table 5.6: Laminated $[0/90]_s$ properties of composite Skin	86
Table 5.7: Comparison of measured and modeled M1 bat properties	86
Table 5.8: Comparison of measured and modeled M2 bat properties	87
Table 5.9: Properties of cricket bat and FEA used in the performance comparison	91

LIST OF FIGURES

Figure 1.1: Cricket field, pitch and wickets	3
Figure 1.2: Different kind of cricket shots	3
Figure 1.3: Oldest cricket bat dated 1729	4
Figure 1.4: Various shapes of cricket bats used since 1729	5
Figure 1.5: Cricket bat terminology	6
Figure 3.1: Cricket balls used in test, first-class and one-day international cricket matches	30
Figure 3.2: Cricket ball test schematic.....	31
Figure 3.3: Cannon accumulator tank, breach plate, and barrel	32
Figure 3.4: The sabot, cricket ball and the supporter.....	33
Figure 3.5: Cannon arrestor plate, light gates, rigid plate, and load cells.....	33
Figure 3.6: Load cells	34
Figure 3.7: Hysteresis plot of cricket ball impacting at 70mph.....	38
Figure 3.8: Cross sectional view of cricket ball Ba and Bb.....	39
Figure 3.9: The average COR and dynamic stiffness of model Ba and model Bb.....	39
Figure 3.10: Comparison between the dynamic properties of Ba and Bb	40
Figure 3.11: Average COR and DS as a function of increasing speed.....	41
Figure 3.12: Linear and non-linear stiffness of the cricket ball impact at different speeds.....	42
Figure 3.13: Comparison of COR for Ba and Bb models (6 balls at each point).....	43
Figure 3.14: Representative force-displacement curves for Ba seam impacts	43
Figure 3.15: Representative force-displacement curves for Ba face impacts.....	44
Figure 3.16: Force-displacement curve for Bb face impacts	44
Figure 3.17: Force-displacement curve for Bb seam impacts.....	45
Figure 3.18: Static and dynamic stiffness of cricket balls	46
Figure 3.19: Face and seam static compression of ball model Ba and Bb.....	47
Figure 3.20: Seam compression of the cricket ball.....	47
Figure 3.21: Face compression of the cricket ball	48

Figure 4.1: Dimensions of cricket bat according to Law 6.....	51
Figure 4.2: Experimental apparatus used to measure the MOI of the cricket bat.....	53
Figure 4.3: Experimental test fixture used to test cricket bats.....	55
Figure 4.4: Pivot assembly used to test cricket bats.....	56
Figure 4.5: Drag coefficient vs. BBS of the cricket ball.....	58
Figure 4.6: Maximum distance travelled by the ball launched at 35 degree with 500rpm and with velocity of 70mph.....	59
Figure 4.7: Comparison between the initial velocity and the distance travelled by a cricket ball.....	59
Figure 4.8: Bat performance curve of E2.....	60
Figure 4.9: Average performance between knocked and unknocked bats.....	61
Figure 4.10: Average performance between English willow and Kashmir willow after knock-in and oiling.....	62
Figure 4.11: BBS as a function of MOI for English and Kashmir willow bats.....	63
Figure 4.12: Cricket bat bending stiffness test.....	64
Figure 4.13: Average stiffness results from 3-point bend tests.....	64
Figure 4.14: Comparison of cricket bat with and without composite skin.....	65
Figure 5.1: Dynamic stiffness apparatus modeled in LS-DYNA.....	73
Figure 5.2: A plot of ball speed vs. time.....	73
Figure 5.3: Force vs. time plot coarse.....	74
Figure 5.4: Fine mesh of cricket ball dynamic stiffness test (12096 elements).....	76
Figure 5.5: Force vs. time curve of fine mesh.....	76
Figure 5.6: Comparison of finite element and experiment of cricket ball impacting a load cell at $v_b = 60\text{mph}$ (26.8 m/s).....	77
Figure 5.7: β vs. COR and dynamic compression.....	78
Figure 5.8: Long time shear modulus G_1 vs. COR and dynamic compression.....	79
Figure 5.9: Bulk modulus (k) vs. COR and dynamic compression.....	79
Figure 5.10: Representative force-displacement curve of B_b for experiment and FEM model.....	80
Figure 5.11: Comparison of COR between average of dozen balls and FEA model as a function of incoming speed.....	81

Figure 5.12: Comparison of the dynamic stiffness between the average of 12 balls and FEA model as a function of incoming speed	81
Figure 5.13: Traditional design (M1) Bat model	83
Figure 5.14: Faceted design (M2) bat model	84
Figure 5.15: Principal axis of wood	85
Figure 5.16: Experimental validation of the M1 model at different impact locations.....	88
Figure 5.17: Representative performance curves for bat and model	88
Figure 5.18: MOI of the bat model when weight was added at different locations.....	89
Figure 5.19: BBCOR as a function of weight location from the pivot.....	90
Figure 5.20: Comparison of finite element model and cricket bat with and without composite skin.....	91

CHAPTER 1

-INTRODUCTION-

The origin of cricket as a sport is not clear; though some theories exist that suggest its origin. There was reference to a game much like cricket played in the 13th century called club-ball. The oldest match recorded was at London in the year 1746 [1.1]. Gambling over matches helped the sport gain popularity throughout the British colonies. In the 18th century, cricket moved out of the colonies to other parts of the globe [1.2]. During this time, the game developed from a British recreational sport into a professional game, and is now played in most of the commonwealth nations.

The cricket field consists of a roughly elliptical or circular shaped grassy ground ranging from 450 feet (150 yards) to 500 feet (167 yards) in diameter as there is no fixed dimensions. Generally the rope is placed on the outer circle of the field to mark a boundary. The starting point of most of the action takes place at the pitch, which is aligned along the long axis of the ellipse. The pitch is carefully prepared rectangle measuring 22 yards long with short grass over hard packed earth as shown in Fig.1.1. On each end of the pitch three wooden posts 1 inch in diameter and 32 inch high, are placed into the ground. Two wooden crosspieces known as bails, are placed on top of the stumps. As shown in Fig.1.1, the set of three stumps and two bails are collectively known as the wicket. The crease are the white lines which measured 4 feet from the wickets, drawn on the both ends of the pitch. Four kinds of creases (one bowling crease, one popping crease and two return creases) are drawn at end of the pitch around the wickets.

The batsman who faces the bowler is the striker and the batsman on the other end of the pitch is non-striker.

The order in which a team bats is determined by tossing a coin. The captain of the winning toss team decides whether to bat or to field. Each team takes turns to bat and field. Each turn is called an inning. The game progresses by bowling the balls in overs. An over is a set of six legal balls (illegal balls are no-ball or wide ball) bowled in succession by single bowler. In case of injury, other teammate can deliver the remaining legal balls for that particular over. The fielding team captain decides which bowler will bowl any given over with a restriction that no bowler can bowl two overs in succession.

A good batsman is a player who protects his wicket but at the same time scores runs. The run is the basic unit of scoring in the game of cricket. The batsman generally plays in and out of the crease to make runs. The common way of making runs is when the striker hits the ball and the batsman runs from one end of the crease to the other without getting out. The batter is out if the fielding team hits the wicket with ball before the batsman crosses the crease. Batsmen also score four or six runs by hitting the ball to or over the boundary. The act of hitting a cricket ball is called a shot. There are different kinds of shots that a batsman can play in order to score runs; Fig.1.2 presents a few of them. The fielding team attempts to end the inning either by getting all the batsman out or completing the specified number of overs (depends upon the conditions chosen before the game). The teams with most runs wins the game.

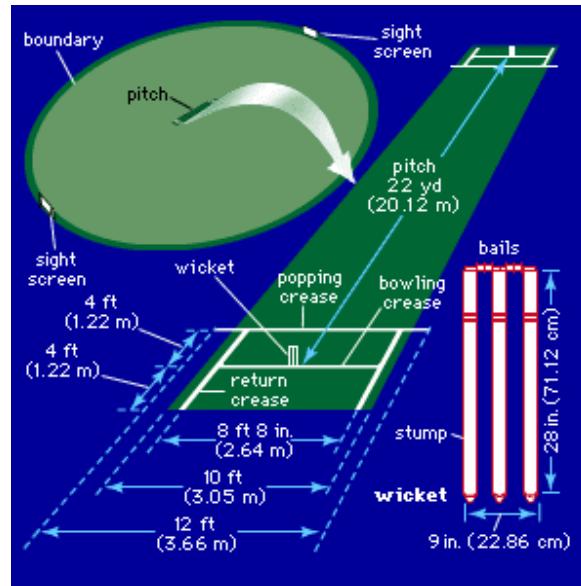


Figure 1.1: Cricket field, pitch and wickets [1.3].



Figure 1.2: Different kind of cricket shots.

Three types of cricket matches are played at the international level: the traditional five-day test match, the one-day international match (ODI), and the 20-20 match. In the traditional five-day test match each team plays two innings and there is no limitation of the number of overs. The ODI is a limited over match where each team is constrained to fifty overs with one inning for each team. The 20-20 match has twenty overs for each team and the game is completed in a few hours. First class cricket is for domestic

matches, with the same conditions as traditional five-day test match. Presently there are more than 100 countries where cricket is played professionally. However, there are only 12 countries who have acquired test match playing status [1.6].

Vital to all the three formats of the game of cricket is the equipment used by the players. Initially, the shape of the cricket bat was more like a hockey stick as shown in Fig 1.3. Since then the cricket bat has been changed various times. Fig 1.4 shows various models of cricket bats that have been used in the game. When the Australian batsman Dennis Lillee emerged onto the field in 1979 carrying an aluminum bat, there was no rule against using it. The bat was not allowed on the grounds because the bat was damaging the cricket ball [1.6]. After that incident a new rule was implemented that the blade of the bat must be made of wood.



Figure 1.3: Oldest cricket bat dated 1729 [1.4].



Figure 1.4: Various shapes of cricket bats used since 1729[1.5].

The cricket bat consists of a handle, shoulder, blade and toe as shown in Fig.1.5. Until recently, the quality of the cricket bat was based only upon the grain structure of the face of the blade. Little research has been done to study the performance of the cricket bats. There is no rule governing the weight of the bat. The modern tendency is to use heavy bats since most batsman believe that a heavier bat allows them to hit the ball further. Batting is the one of the most exciting parts of the game for cricket fans.



Figure 1.5: Cricket bat terminology [1.3].

The blade of the bat is commonly made of Kashmir or English willow. English willow is considered superior to Kashmir willow, even though there is no scientific difference between the species. Bat performance also depends on the properties of the ball. The aerodynamics of cricket balls has been studied extensively, but little has been published regarding its impact response. Research on softballs and baseballs show that the properties of balls can have large effect on the performance of the bat.

Cricket laws require that the blade of the cricket bat be made of wood. There is no law regarding the material on the backside of the blade, however. Composite materials are now extensively used in sports such as softball, tennis, golf, and baseball. Kookaburra cricket bat manufactures has added a composite skin on the back of the blade to increase durability. The effect of the composite skin will be experimentally and computationally investigated in this study.

Given the age and popularity of the game surprisingly little research has been done to advance the equipment. The following study will consider the effect of weight distribution, wood species, composite skin and the ball on bat performance.

Reference:

- [1.1] Grace, W. C. "Cricket" Simpkin, Marshall, Hamilton, Kent and Co. Limited, 1891.
- [1.2] Bowen, R. "Cricket: a History of Its Growth and Development throughout the World" London, Eyre and Spottiswoode, 1970.
- [1.3] Image copied from: <http://www.britannica.com>
- [1.4] Image copied from: http://en.wikipedia.org/wiki/Cricket_bat
- [1.5] Image copied from: <http://www.liveindia.com/cricket/Batting.html>
- [1.6] www.cricinfo.com

CHAPTER 2

-LITERATURE REVIEW-

2.1 Ball Response

2.1.1 Coefficient of Restitution

2.1.1.a Definition and History

The impact between two objects or balls is always followed by a loss of energy. The coefficient of restitution e is defined as the ratio of the relative velocity of the colliding objects after and before impact, [2.1] and is expressed as

$$e = \left(\frac{v_2 - v_1}{V_1 - V_2} \right) \quad (2.1)$$

where v_1 and v_2 are the velocities after impact, V_1 and V_2 are velocities before impact, and the subscript refers to object 1 and 2. The coefficient of restitution is often measured from a high-speed impact with a massive, rigid, flat wall of either wood or metal [2.2]. If one object is rigid, the coefficient of restitution can be expressed by

$$e = \frac{-v_1}{V_1} \quad (2.2)$$

When there is no energy loss we have the perfectly elastic collision or $e=1$, and for completely an inelastic collision $e=0$.

For two colliding objects the coefficient of restitution depends upon the velocity of approach, the material and the geometry of the objects. Hodgkinson (1834) showed

that the coefficient of restitution decreased with increasing relative velocity. Raman showed $e \rightarrow 1$ as $v \rightarrow 0$ and Vincent showed that $e \rightarrow 0$ as $v \rightarrow \infty$ [2.4]. Raman used a photographic system to examine the very low approach velocity impacts between polished spheres of brass, aluminum, bronze, white marble and lead where Vincent conducted the experiments at high impact velocity up to 40 m/s.

Cochran, Smith, Duris and Chauvin [2.6], [2.7], [2.8], [2.9] also showed the COR decrease with increasing speed for sports balls. Chauvin explained that rebound speed of a ball is reduced because energy is expended, deforming the ball during impact. A material that loses energy as it deforms will expend increasingly more energy with greater deformation and speed.

Stensgaard and Laegsgaard [2.11] summarized the energy loss mechanisms of a steel ball and a flat block, into three groups:

- (a) excitation of internal waves or vibration modes in the rigid block or in the ball
- (b) plastic deformation of the ball or rigid block
- (c) viscoelastic behavior of the rigid block or the ball.

Li stated that less than 4% of the total impact energy is assigned to the propagation of elastic waves when a sphere impacts a rigid wall [2.51]. During the bat-ball impact there is no noticeable damage to the ball. This leaves viscoelastic behavior of the ball as the primary source of energy dissipation [2.11].

2.1.1.b COR Models

Suppose that two balls with masses m_1 and m_2 collide with velocities v_1 and v_2 respectively. After, collision let m_1 recoil with velocity v_1 and m_2 with velocity v_2 . Consider a frame of reference where the center of mass is at rest and the total momentum remains zero. The total initial kinetic energy E_i and final kinetic energy E_f are [2.3]

$$E_i = \frac{1}{2} m_i v_i^2 \left(1 + \frac{m_1}{m_2} \right) \quad \text{and} \quad E_f = \frac{1}{2} m_1 v_1^2 e^2 \left(1 + \frac{m_1}{m_2} \right) \quad (2.3)$$

The fractional energy loss f , which is the ratio of the kinetic energy to the initial kinetic energy is

$$f = 1 - e^2 \quad (2.4)$$

Hodgkinson [2.12] modeled contact between bodies where linear springs represent the local compliance of deformation of the small region of contact of each body. Hodgkinson showed that contact forces can be related to the compression x_i in each spring, as

$$\frac{F_i}{k_i} = x_i \quad (2.5)$$

where F_i is positive in compression and k_i is the spring stiffness. The total compression in the system can be written as:

$$x_{tot} = k_*^{-1} F \quad (2.6)$$

where

$$k_*^{-1} = (k_1^{-1} + k_2^{-1}) \quad (2.7)$$

is the sum of the different stiffness and k_i are the stiffness of each material, and a value proportional to Young's modulus $k_i \sim E_i$ or yield strength $k_i \sim Y_i$ is suggested. When materials with different stiffness collide, they contribute to the overall COR in proportion to their relative compliances, which lead to an equation of composite COR [2.12]

$$e_* = \frac{k_2 e_1 + k_1 e_2}{k_1 + k_2} \quad (2.8)$$

where e_1 and e_2 are the COR of each material.

Coaplen [2.13] further extended the work of Hodgkinson by introducing an energetic COR, defined as the square root of the ratio of work done by the normal contact force during restitution, W_r , to the work done by the normal contact force during compression, W_c .

$$e_*^2 = -\frac{W_r}{W_c} \quad (2.9)$$

This connotes that e may consist of two phases: an initial period of compression when bodies are approaching each other and a period of restitution when bodies are moving apart. When two bodies collide the total work done during compression is sum of the work done by each body, W_{1c} and W_{2c}

$$W_c = W_{1c} + W_{2c} \quad (2.10)$$

using the definition of energetic COR equation (2.10) is expressed as

$$e_*^2 = e_1^2 W_{1c} + e_2^2 W_{2c} \quad (2.11)$$

where e_* is the composite COR and e_i is the COR for each body. The energy stored at the end of the compression phase of each body can be found by assuming linear constitutive behavior, and is the product of spring stiffness and square of compression on each spring. The total energy stored in the system at the end of the compression phase is

$$W_c = \frac{k_1 x_1^2 + k_2 x_2^2}{2} \quad (2.12)$$

Following Newton's third law Coaplin arrived at

$$e_*^2 = \frac{k_1 e_2^2 + k_2 e_1^2}{k_1 + k_2} \quad (2.13)$$

Equation 2.8 and 2.13 describe a system COR as a function of the individual COR and stiffness of the impacting bodies. Equation 2.13 is generally preferred since it was developed from energy considerations, while equation 2.8 is an empirical relation. The rate dependence of the ball complicate measuring its stiffness. In the following we will present a method to measure ball stiffness under deformation rates representative of play. This will improve the estimate of system COR through equations like 2.13.

2.1.2 Dynamic Ball Hardness

Most of the work on ball hardness has been towards human safety. Ball hardness can be quantified through a so called dynamic stiffness, which can be viewed from the perspective of the impact force. This can be found by firing a ball at a rigid wall and measuring the impact force [2.14]. The unknown ball displacement can be replaced by the measured force, assuming the ball acts as a non-linear spring during the loading phase [2.15] according to

$$F = kx^n \quad (2.14)$$

where k and n are the unknown spring constants and F and x are the force and displacement of the spring respectively. Equating the initial kinetic energy of the ball to the potential energy at maximum deformation during impact and solving for k we obtain:

$$k = \left[\frac{2}{m_b(n+1)} \right]^n \frac{F_p^{n+1}}{v_i^{2n}} \quad (2.15)$$

where m_b is the ball mass, F_p is the peak impact force, and v_i is the incoming ball speed. Smith [2.16] assumed the ball to act as a linear spring during deformation ($n=1$), so the stiffness reduces to:

$$k = \frac{1}{m} \left(\frac{F}{v_p} \right)^2 \quad (2.16)$$

Hendee [2.17] demonstrated that higher impact velocities yield higher peak forces. Impact force increased by an average of 448% when the impact velocity was increased by 200%. Smith [2.9] found a decrease of 6.5% in the dynamic stiffness if the ball is fired against rigid cylindrical surface rather than flat surface. Carre [2.18] showed that in the case of cricket balls as the impact velocity increased, the peak force and deflection was also increased. The stiffness (found by drop testing and static compression) was relatively constant.

Giacobbe and Scarton [2.19] introduced another method to measure the dynamic hardness. A variety of sports balls were dropped from a known height on to three piezoelectric force transducers attached to impact plate. The frequency (Hz) where the

power spectrum level dropped to -60 dB corresponded to a force amplitude drop of one half and was called the Scarton Dynamic Hardness (SDH) [2.19]. The slope of the power spectrum at the SDH point was called the DSDH, where D stands for derivative. The DSDH is always negative and is defined as

$$DSDH = \frac{-\gamma}{SDH} \quad (2.17)$$

Rearranging

$$\gamma = -(SDH)(DSDH) \quad (2.18)$$

where he found that γ is a function of the damping coefficient ξ ;

$$\xi = \frac{1}{\sqrt{1 + \left(\frac{\pi}{\ln(COR)}\right)^2}} \quad (2.19)$$

which can be solved for a known value of COR as

$$COR = e^{\frac{-\pi\xi}{\sqrt{1-\xi^2}}} \quad (2.20)$$

Scarton's [2.19] method was used to measure the dynamic hardness for a wide variety of balls including tennis, golf, softballs, baseballs and hockey pucks.

2.1.3 Construction of Cricket Ball

Every sport ball is made of different materials with different construction. In some cases the difference in the construction of the samples of the same brand can be seen clearly, which affects their mechanical properties. There is very little information

available regarding the effect of construction of the cricket ball on its properties. Nicholls [2.20] used a uniaxial compression test for baseballs to show that when a ball positioned in a “cover” orientation the force-displacement curve and peak force is greater than on a “seam” orientation.

Carre and Haake [2.18] used impact testing where a cricket ball was dropped on load cells from different heights at a speed of 13 mph and quasi-static testing. They found that the ball deforms more with impacts landing on the seam than impacts landing perpendicular to seam. This information is important as it can help reduce the severity of impact injuries on the players. It is important to note the impact speed used is much lower than the actual playing conditions.

Another study done by Hendee, Greenwald and Crisco [2.17] showed that the peak force of impact at 60 mph for a traditional baseball is 2.4 times higher than the peak force of a modified (softer) baseball. The COR of the modified (softer) ball also decreased more rapidly with increasing impact velocity than the traditional ball.

Fuss [2.22] used a quasi-static compression test on different kinds of cricket balls. Each ball was loaded up to 9 kN with crosshead speeds of 500, 160, 50, 16, and 5 mm/min. He found that balls with uniform construction have higher stiffness than other balls. The results show that balls with rubber cores are less stiff than balls with a cork core at its center.

2.1.4 Ball Model

Several people have used different methods for ball modeling. Sandmeyer [2.26] used a trial and error method from a known ball COR and contact time with finite

elements. Rate effects were neglected. Mustone and Sherwood [2.23] used a Mooney-Rivlin material model in LS-DYNA, which accepts the load-displacement curve from static testing performed at different speeds. Bathke [2.24] used ABAQUS to determine the properties of the ball numerically. A quasi-static compression test was used to determine the elastic properties of the components of each layer of the baseball. Although the layers were elastic, the COR decreased linearly with increasing speed. The speed effect may be due to a loss in energy to internal vibrations within the baseball. The coefficient of restitution was too high in his model.

Smith, Shenoy and Axtell [2.25] selected a viscoelastic model for a baseball using LS-DYNA. The time dependent shear modulus was defined as

$$G(t) = G_{\infty} + (G_0 - G_{\infty})e^{-\beta t} \quad (2.21)$$

and a constant bulk modulus, k where G_0 is the instantaneous shear modulus and G_{∞} is the long term shear modulus. Quasi-static testing was used to find the long term shear modulus whereas constants G_0 and β were found by fitting the experimental load-time curve. The G_{∞} was found by

$$G_{\infty} = \frac{E}{2(1+\nu)} \quad (2.22)$$

where E and ν were found by static tests. The experimental and finite element results for COR and dynamic stiffness correlated well [2.14].

Duris [2.9] used Dynamic Mechanical Analysis (DMA) to model the COR and dynamic stiffness of softballs. Rectangular coupons were machined from the ball core

using a circular saw and milling machine. He used a Prony-series viscoelastic material model within LS-DYNA defines as

$$G(t) = \sum_{i=1}^N g_i e^{-\beta_i t} \quad (2.23)$$

where g_i and β_i are the shear moduli and the decay constant, respectively. The results did not agree well with experimental results. The COR and dynamic compression were observed to be 100% and 50% higher respectively than experimental results.

2.2 Bat Response

2.2.1 Bat Performance metrics

The appraisal of cricket bat performance depends upon many factors. Grant [2.30] gave five parameters that are needed to determine the bat performance:

The point of impact on the bat

The pre-impact speed of the ball

The pre-impact speed of the bat

The post-impact speed of the ball

The post-impact speed of the bat

The bat with the higher coefficient of restitution will produce a ball with the greatest post-impact speed. The focus of manufactures has been to improve the COR of the bat.

Fisher [2.31] found that the position of the maximum COR for a cricket bat lies between 0.19 and 0.23m from the free end of the bat. The bat was impacted at every 0.06m for 9 impact locations where each impact location experienced 6 direct impacts.

The position closest to the free end had very low COR. The initial speed used for this study was 9m/s (20mph) which was lower than actual playing conditions.

Bryant [2.35] claimed that there is an effective area where performance of the bat is maximum. The tests involved six collegiate baseball players, the pitch speed was relatively constant in a range of 54-59mph. 180 hits on each bat were measured, and the mean hit-ball speeds were 88.6mph for wood bats and 92.4mph for aluminum bats.

2.2.2 Field Conditions

Bowlers use three kinds of bowling deliveries [2.10]: fast bowling, medium pace or swing bowling and spin bowling. Fast bowlers deliver the ball at speeds in excess of 80mph where the mean ball speed at release is 86mph. Medium paced or swing bowlers deliver the ball between 65mph and 80mph with a mean ball release speed of 73mph. Spin bowlers deliver the ball at 40mph and 60mph with a mean ball release speed of 51mph. Justham [2.10] noted that the fastest average speed occurs in test match and slowest average speed occurs at 20: 20 match.

The motion of the cricket bat is similar to that baseball or softball bat. Adair [2.32] showed that the swing of the baseball bat is very complex and consists of a combination of translation and rotation. For a particular input energy these two values describe the swing speed of player. Fleisig [2.33] conducted tests including 16 baseball collegiate batters with bat weight varying from 28-32 ounces. Bat motion was analyzed for 2 frames before impact where the average swing speed was 52-65mph or 1940-2720 degrees per second. Bahill and Freitas [2.34] also reported a swing speed as 55-63 mph for a college softball batter swinging the bat at imaginary ball.

Nicholls [2.36] studied the effect of bat moment of inertia on ball exit velocity. The study included 17 (10 right handed and 7 left hander) participants from the Australian baseball league. Each player hit with both wood and metal bats. High-speed video was collected using an electronically synchronized 200-Hz camera. Results revealed that the bat exit velocity was 6.5% lower for wooden bats which had 22% higher MOI than the metal bats.

More impulse is required to change the bat speed or direction as the MOI is increased. Therefore, greater MOI compromises the batsman's ability to control the path and bat velocity as it swings towards the ball. A field study conducted by Smith [2.38] on mass and moment of inertia involved 16 amateur slow-pitch softball players of two skill levels. The study included two groups of bats where one group had constant weight and other group had constant MOI. The average pitch speed was 23mph. The bat mass and MOI in this study ranged from 24.5 – 31 oz and 7000 – 11000 oz-inch², respectively. Bat swing speed had an observable dependence on the bat MOI, while it was independent of the bat weight.

A recent study conducted by Cross [2.40] supports Smith's research on the effect of bat mass and MOI on swing speed. Six different rods were used, where three rods had the same swing mass but their MOI differed by a factor of 11. The other three rods had the same MOI but differed in swing mass by a factor of 2.7. The length was varied to achieve the large variation. It was found that swing speed decreased with increasing MOI. It was shown that the bat mass had only a small effect on the swing speed.

Another study on swing speed was conducted by Koenig [2.39] swinging a bat at both a pitched and stationary ball. Bat speeds varied from 43.5 – 79.5mph. A 10% increase in MOI produced a 4mph decrease in bat swing speed.

2.2.3 Bat Composition

Advanced materials help improve bat performance without violating the rules of the game. Such advancements, together with use of stiff and lightweight composite materials, have engendered many designs. Innovation is limited in cricket where the rules insist that the blade be made of wood [2.41].

Bryant [2.42] showed that the performance of wooden bat is lower than aluminum bats. A similar study was done by Greenwald [2.43] on two aluminum bats and wooden bats. The hit-ball speed of the wood bats exceeded 101mph whereas the aluminum bat exceeded 106mph. Similar results were found by Shenoy [2.25].

A recent study was done by Stretch [2.44] to compare the rebound characteristics of wooden and composite cricket bats. In this study two composite, three English willow and one Kashmir willow bats having similar weight and shape were compared at impact speeds of 42, 63 and 81 mph. It was found that the average rebound speed of the composite bats was lower than the traditional willow bats at all the three incoming speeds. The rebound speed of the Kashmir willow was almost 20% lower than the traditional English willow at all the three approaching speeds.

Most of the modern cricket bat designs are ineffective at increasing the frequencies of flexural vibration. The factors that might make significant improvement in bat performance are[2.41]:

1. Increasing the diameter of the handle
2. Removing the damping material (rubber strips) from the handle
3. Increasing the thickness of the bat

A recent study was conducted by Hariharan [2.37] on bat performance with various impact combinations. Model analysis was used to determine the region where the maximum ball exit velocity was located. It was found that the region for maximum ball exit velocity in the finite element model was between 0.72m and 0.8m from the top of the bat.

2.2.4 Bat Numerical Model

A study was conducted by Zandt [2.45] to determine the hit-ball speed or batted-ball speed and bat behavior. A numerical method was developed to represent the bat as a series of slices. A comparison of a rigid, and elastic bat with only the first mode of vibration was conducted. It was concluded that the first mode of bat vibration was the dominant mode. This method was further used by Cross [2.46] in which an aluminum beam was used, which also showed that the first mode of vibration was the dominant mode.

Shenoy [2.25] used LS-DYNA to model the dynamic interaction of a bat and ball. The model consisted of 8-noded solid elements for the ball and wooden bat. Four-noded Hughes Liu shell elements were used for the aluminum bat. The numerically obtained hit-ball speeds correlated well with those obtained experimentally. Penrose [2.47] used two different methods involving finite element bat/ball models. In the first model isotropic properties are used for bat. The ANSYS/LS-DYNA package was used for second model

of a bat/ball impact where two basic designs were modeled for comparison. Orthotropic properties were used as the bat material. The two methods showed good correlation with each other.

John [2.48] studied the deflection of cricket bats experimentally and numerically. His experimental work involved modal analysis with a clamped handle. His numeric model constrained the proximal end of the bat. The bat vibrational frequency was measured from ball impacts in the numerical model and compared with experiment. The FEM model showed good agreement with experimental results, suggesting that the FEM model is a feasible numerical tool to predict the performance of a cricket bat. It was observed that the performance of the bat varied with impact location.

Grant [2.41] used a finite element model to compare the performance of a variety of designs. The basic model was correlated to experimental data. Agreement improved when the density of the wood was increased by 50% from that found in the literature. It was observed that the mode one and two frequencies were identical whereas third mode was 4% lower.

2.2.5 Bat Constraint

Constraint is an important factor to determine bat performance. Brody [2.49] used two softballs, one wood and one-aluminum bat to experimentally measure vibration. Comparison of the vibrational response between freely, hand held and vice clamped bats was done. The freely suspended bat had the same vibrational response as the hand-held bat but there was a difference in the vibrational response in the clamped bat. He

concluded nevertheless that grip firmness should not determine the post-impact velocity of the ball.

Fisher [2.50] measured the hand loads on five different commercial bats. Three clamping configurations were employed on rigid clamps, in a hand simulator, and hands of a human subject. The clamps were positioned 210mm apart and rigid clamps were tightened to 300N, whereas hand the simulator was tightened to 8 N, equal to human grip force. The impact positions were at 6cm intervals from the end of the bat, impacted from a ball drop tube at 9m/s. He found that the hand simulator clamped loads were very similar in distribution to hand loads, for the load measured along the length of the bat. It was also observed that the rigid clamped grip load was ten times the magnitude of the hand-held bat.

Weyrich [2.51] used aluminum and wooden bats to study the effect of grip firmness and bat composition. Bats were clamped in a vise or freely suspended. Three impact locations were used: center of percussion, center of gravity and the end of the bat. The rebound velocities for impacts at the center of gravity for the wooden bat were the same for clamped and freely suspended constraints. It further signifies that the constraints do not affect the performance of the bat.

2.3 Summary

The purpose of this chapter was to review the historical and current research relevant to bat performance. In doing so, ball and bat testing methods have been discussed. Experimental and finite modeling methods have been explained. The most significant contribution revolves around finite element modeling of cricket balls and bats.

In the following chapters, experimental bat and ball testing along with numeric modeling will be presented. The dynamic properties of the ball has a great effect on the performance of the bat. The variation in construction which effects the dynamic response of the cricket balls will be discussed in the following chapter. Comparison between different types of wood species and composite materials will be conducted. An extensive study regarding the ball and bat finite element models will be carried out and verified with experimental results. The effect of weight distribution on the bat finite element model will also be studied.

REFERENCE

- [2.1] Barnes, G. "Study of collisions". Am. J. Phys. **26**, p. 5-12. 1957.
- [2.2] ASTM F 1887-02. "Standard test method for measuring the coefficient of restitution of baseballs and softballs." West Conshohocken, Pa. 2003.
- [2.3] Cross, R. "The coefficient of restitution for collisions of happy balls, unhappy balls, and tennis balls". Am. J. Phys. **68** (11), p. 1025-1031. 2000.
- [2.4] Barnes, G. "Study of collisions". Am. J. Phys. **26**, p. 5-12. 1957.
- [2.5] Brody, H. "The physics of tennis. III. The ball-racket interaction". Am. J. Phys. **65** (10), p. 981-987. 1997.
- [2.6] Chauvin, D.J., Carlson, L.E. "A comparative test method for dynamic response of baseballs and softballs. International Symposium on Safety in Baseball/Softball". ASTM STP 1313, p. 38-46. 1997.
- [2.7] Cochran, A.J. "Development and use of one dimensional models of a golf ball". J. Sports Sciences. Taylor and Francis, Ltd. London, UK. 2002.
- [2.8] Strangwood, M., Johnson, A.D.G., Otto, S.R., "Energy losses in viscoelastic golf balls". Proc. IMechE, Vol.220 Part L, Journal of Materials: Design and Applications, pp. 23-30. 2006.
- [2.9] Duris, J.G and Smith, L.V. "Evaluation test methods used to characterize softballs". The Engineering of Sport 5, Vol 2, pp. 80-86. ISBN: 0-9547861-1-4. Davis, CA. 2004.
- [2.10] Justham, L.M., West, A.A., Cork, A.E.J., "An Analysis of the differences in bowling technique for Elite Players during International Matches" The impact of technology on Sports,pp.331-336. 2007
- [2.11] Stensgaard, I., Laegsgaard, E. "Listening to the coefficient of restitution-revisited". Am. J. Phys. **69** (3), p. 301-305. 2001.
- [2.12] Hodgkinson, E. "On the collision of imperfectly elastic bodies". Report of the fourth Meeting of the British Association for the Advancement of Science. 1835.
- [2.13] Coaplen, J., Stronge, W.J., Ravani, B. "Work equivalent composite coefficient of restitution". Int. J. of Impact Engrg. **30**, p. 581-591. 2004.
- [2.14] Duris, J.G. "Experimental and Numerical characterization of softballs". Master thesis. Washington State University. 2004.

- [2.15] Smith, L.V., Duris, J.G., Nathan, A.M. “Describing the dynamic response of Softballs” Unpublished.
- [2.16] Smith, L.V., Biesen, E. “Describing the plastic deformation of aluminum softball bats”. The impact of technology on Sports, pp.351-356. 2007
- [2.17] Hendee, S.P., Greenwald, R.M., Crisco, J.J. “Static and Dynamic properties of various baseballs”. J. App. Biomech. **14**, p. 390-400. 1998.
- [2.18] Carre, M.J., James, D.M., Haake, S.J. “Impact of a non-homogeneous sphere on a rigid surface”. Proceeding of the institution of Mechanical Engineers, Journal of Mechanical Engineering science. Vol. 218 Part C: pp. 273. 2004
- [2.19] Giacobbe, P.A., Scarton, H.A., Lee, Y.S. Dynamic hardness (SDH) of baseballs and softballs. International Symposium on Safety in Baseball/Softball. ASTM STP 1313, p. 47-66. 1997.
- [2.20] Nicholls, R.L., Miller, K., Elliott, B.C., “Modeling deformation behavior of the baseball”. Journal of applied biomechanics. pp. 18-30. 2005.
- [2.21] Bartel, D.M., Yagley, M.S., Dewanjee, P.K. “Golf ball with high Coefficient of Restitution” United States Patent. Patent No: US 6,648,775 B2, 2003.
- [2.22] Justham, L.M., West, A.A., Cork, A.E.J., “Non-Linear viscoelastic properties and construction of cricket balls” The impact of technology on Sports, pp.331-336. 2007
- [2.23] Mustone, T.J., Sherwood, J.A. “Using LS-Dyna to characterize the performance of baseball bats”. Unknown source.
- [2.24] Bathke, T. “Baseball impact simulation”. Senior mech. eng. thesis, Brown University. 1998.
- [2.25] Smith, L.V., Shenoy, M.M., Axtell, J.T., “Performance assessment of wood, metal and composite baseball bats”. ASME IMECE, 2000.
- [2.26] Sandmeyer, B.J. “Simulation of bat/ball impacts using finite element analysis”. Master’s thesis, Oregon State University. 1994.
- [2.27] Bowen, R., “Cricket: A History of its growth and development throughout the world”. Eyre and Spottiswoode. London. 1970
- [2.28] The laws of Cricket – 2000 Code, Marylebone Cricket Club, London, 2000
- [2.29] John, S., Li, Z.B. “Multi-directional vibration analysis of cricket bats” The engineering of Sports, 2002

- [2.30] Grant, C., Davidson, R.A. "Design of a Cricket bat test machine" Proceeding of the second international conference on the engineering of sports, Blackwell Science, Oxford, pp41-48, 1998
- [2.31] Fisher, S., Vogwell, J. "The dead spot of the tennis racket" Am. J. Phys. Vol 65, pp 754-764. 1997
- [2.32] Adair, R. K. "The Physics of baseball" 2nd Edition, 1994
- [2.33] Fleisig, G. S., Nigel, Z., David, S., Andrew, J. R., "The relationship among baseball bat weight, moment of inertia, and velocity" Am. Sports Medicine Ins., August 20, 1997
- [2.34] Bahill, A.T., Freitas, M. M. "Two Methods for recommending bat weight" Annals of Biomedical Engineering, pp: 436-444, 1995
- [2.35] Bryant, F. O., Burkett, L. N., Chen, S. S., Krahenbuhl, G. S., Lu, P. "Dynamic and performance characteristics of baseball bats" Research Quarterly Exercise Sports, 1979
- [2.36] Nicholls, R. L., Elliott, B. C., Miller, K., Koh, M. "Bat kinematics in baseball: Implication for ball exit velocity and player safety" Journal of Applied Biomechanics 19, pp: 283-294, 2003
- [2.37] Hariharan, V., Srinivasan, P. S. S. "Inertial and vibration characteristics of a cricket bat" vibrationdata.com
- [2.38] Smith, L., Broker J., Nathan A., "A Study of Softball Player Swing Speed," in: Sports Dynamics Discovery and Application, Edited by Subic A., Trivailo P., and Alam F., (RMIT University, Melbourne Australia), pp: 12-17, 2003
- [2.39] Koenig, K., Hannigan, T., Davis, N., Hillhouse, L. "Inertial effect on Baseball Bat Swing Speed" 1997
- [2.40] Cross, R., Bower, R. "Effects of Swing-Weight on swing speed and racket power" journal of Sports Sciences, pp: 23-30 January 2006
- [2.41] Grant, C. "The role of the materials in the design of an improved cricket bat" MRS Bulletin. March 1998
- [2.42] Bryant, F. O., Burkett, L. N., Chen, S. S., Krahenbuhl, G. S., Lu, P. "Dynamic and performance characteristics of baseball bats" Rec. Q. Exerc. Sport, pp: 505-510, 1979
- [2.43] Greenwald, R. M, Penna, L. H., Crisco, J. J., "Difference in batted ball speed with wood and Aluminum baseball bats: A batting cage study" J. Appl. Biomech., 17, pp: 241-252, 2001
- [2.44] Stretch, R. A., Brink, A., Hugo, J. "A comparison of the ball rebound characteristics of wooden and composite cricket bats at three approach speeds" Sports Biomechanics, Vol 4, pp: 37-46, 2006

- [2.45] Zandt, V. L. L. "The dynamical theory of the baseball bat" American Journal of Physics, February, 1992
- [2.46] Cross, R. "Impact of a ball with a bat or racket" American journal of Physics, August, 1999
- [2.47] Penrose, J. M. T., Hose, D. R. "Finite element impact analysis of a flexible cricket bat for design optimization" The engineering of sports. 1998
- [2.48] John, S., Li, Z.B. "Multi-directional vibration analysis of cricket bats" Proceedings of the 4th International Conference on the Engineering of Sport. Held in Kyoto, Japan, September 3rd-6th, Published in 'The Engineering of Sport 4', Editors Ujihashi S & Haake S J, pp 96-103, 2002. ISBN 0632 06481 1, 2002
- [2.49] Brody, H. "Model of baseball bats" American journal of Physics, August 1990
- [2.50] Fisher, S., Vogwell, J., Ansell, M. P. "Measurement of hand loads and the centre of percussion of cricket bats" Journal of Materials: Design and applications, Proc. IMechE Vol.220, 2006
- [2.51] Li, L-y., Thornton, C., Wu, C-y. Impact behavior of elastoplastic spheres with a rigid wall. Proc. Instn. Mech. Engrs. 214 (C). 2000.

CHAPTER 3

-BALL TESTING-

3.1 Introduction

Cricket balls are made from cork at the nucleus surrounded by several layers of tightly wound string, and covered by a leather case with a slightly raised seam. The covering of the leather case is constructed of four pieces, but the hemispheres are rotated by 90 degrees with respect with each other. The equator of the ball is stitched to form six rows, whereas the remaining two leather seams are hidden stitched. The cricket ball measures between $8 \frac{13}{16}$ and 9 inches (22.4 and 22.9 cm) in circumference and weighs between 5.5 and 5.75 ounces (155.9 and 163.0 g). There are a number of ways to construct cricket balls, with varying core designs [3.1]. Cricket balls are machine or handmade. Conventionally, cricket balls of red color are used in test matches and first-class cricket; whereas white balls are used in one day international cricket matches as shown in Fig. 3.1.



Figure 3.1: Cricket balls used in test, first-class and one-day international cricket matches.

There is little data regarding the impact properties of cricket balls but the impact speed has been measured. Studies showed that the release speed from the bowlers hand is 100mph and the speed at the batting end after rebounding from the pitch is 80mph. The maximum ball velocity at the batter end was recorded in the 1999 world cup Tournament was 93mph [3.2].

3.2 Ball Testing Apparatus

An experimental apparatus has been designed that minimizes the variability in pitch speed, impact location, and spin of the ball. An apparatus was designed in which both the COR and dynamic stiffness of the ball can be measured. A schematic of the test apparatus is shown in Fig. 3.2.

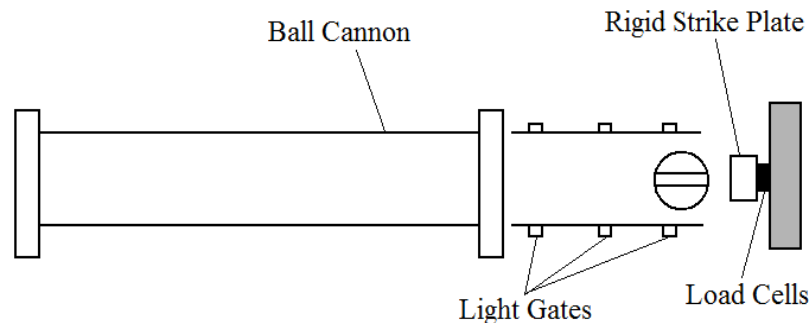


Figure 3.2: Cricket ball test schematic.

The experimental apparatus consisted of the canon, light curtains, load cells, rigid wall and a desktop computer. The canon setup consisted of a large accumulator where the pressure within the air tank was controlled by a regulating valve connected to the computer. The desired pitch speed was achieved by adjusting the pressure in the

accumulator tank. The ball was placed at the breach end of the barrel which closed by pneumatic cylinders. Fig. 3.3 shows the cannon's air accumulator tank, breach plate, and barrel.

A sabot was used to load the ball in the barrel to ensure proper centering and that the ball was not spinning after being fired. The sabot was made of polycarbonate, as shown in Fig. 3.4. On the other side of the barrel an arrestor plate prevented the sabot from traveling in the light curtain, where the ball velocity before and after the impact was measured. Three pairs of ADC light gates (Automated Design) were used to measure the incident and rebound speeds of the cricket balls. The arrestor plate, light gates, rigid plate, and load cells are showed in Fig. 3.5.

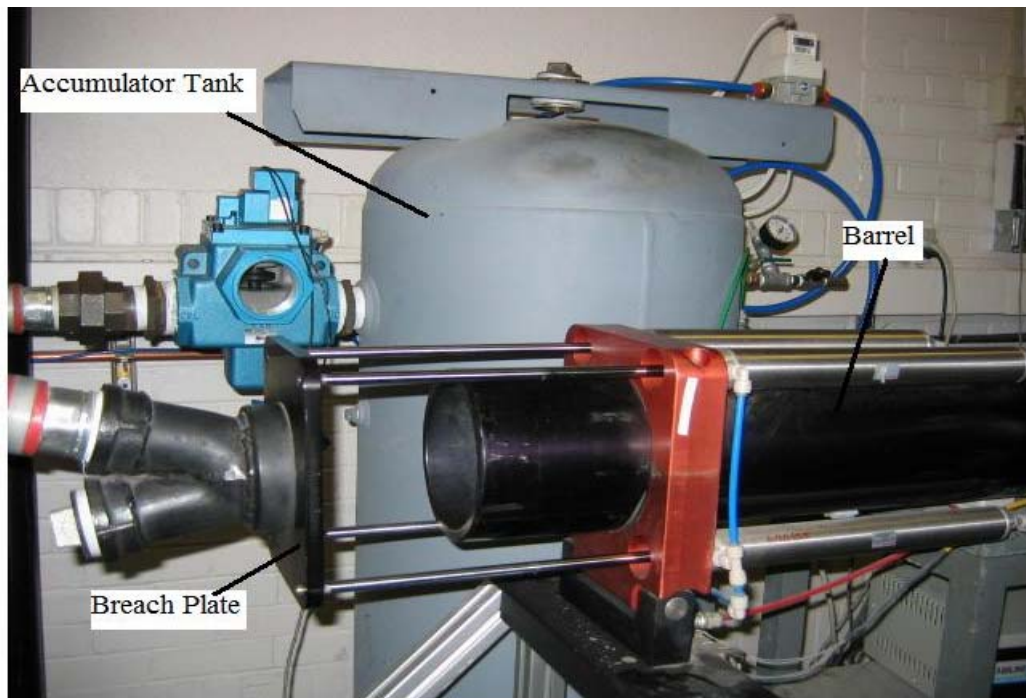


Figure 3.3: Cannon accumulator tank, breach plate, and barrel.

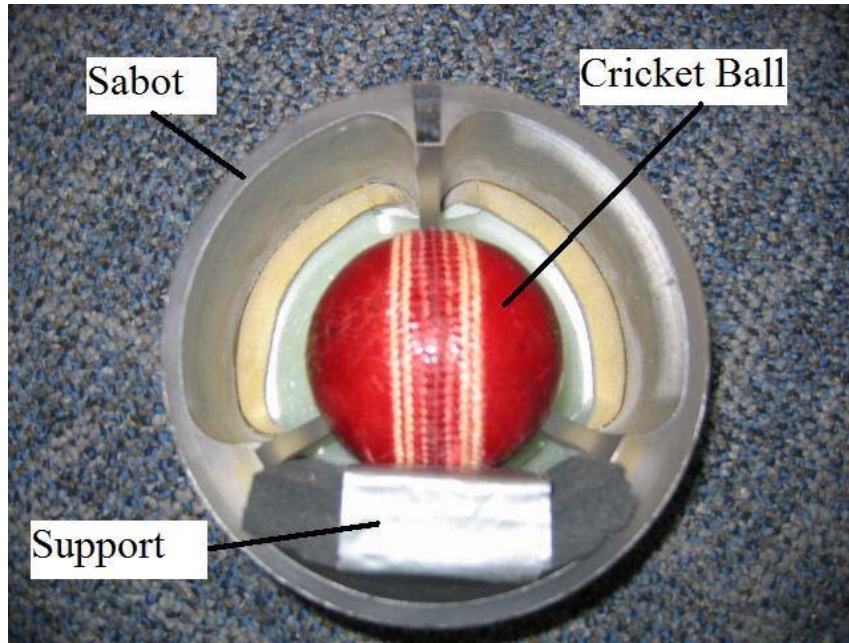


Figure 3.4: The sabot, Cricket ball and the supporter.

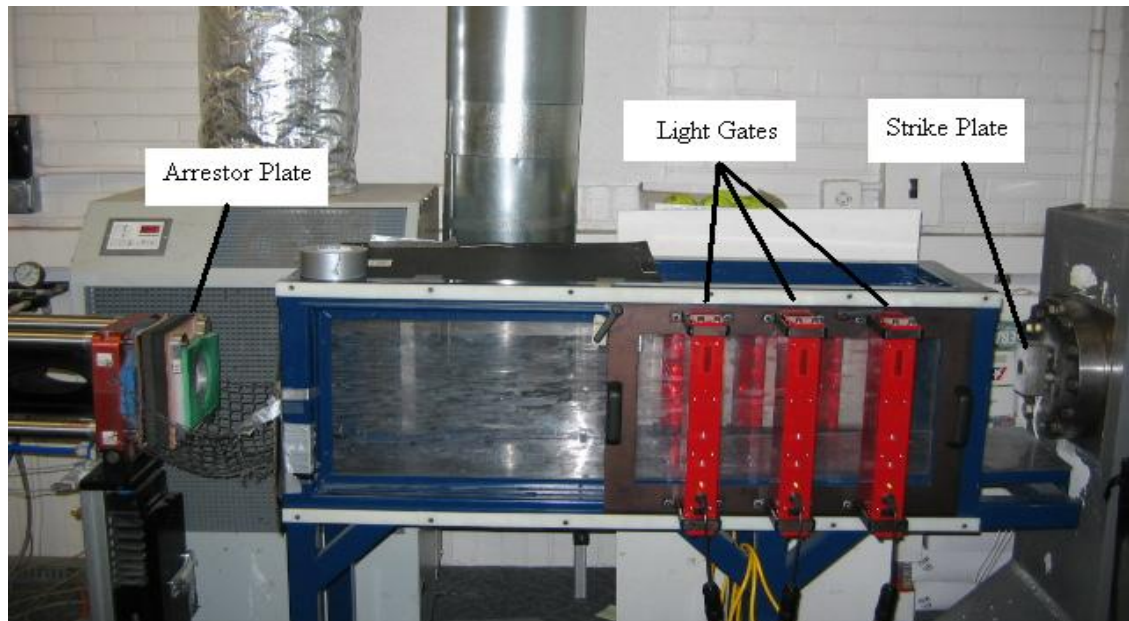


Figure 3.5: Cannon arrestor plate, light gates, rigid plate, and load cells.

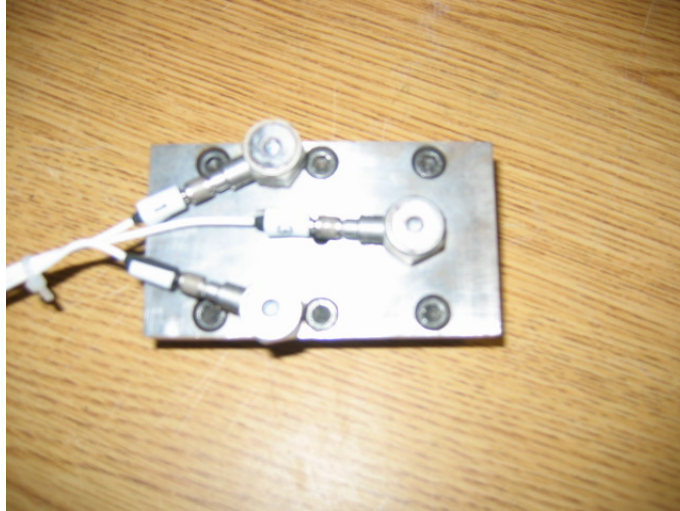


Figure 3.6: Load cells.

Between the solid impact surface and the rigid concrete wall there is a group of three rigidly mounted load cells (PCB Model 208C05). The load cells were arranged in an equilateral triangle with two inch spacing between each cell, illustrated in Fig. 3.6. LabView version 7.1 (National Instruments, Austin, Texas) was used to control the ball speed and impact location on the solid impact surface.

The balls were conditioned at $72 \pm 4^\circ\text{F}$ temperature and $50 \pm 5\%$ relative humidity for 14 days prior to testing. Only impacts were used when the ball rebound after impact was within 5° of the inbound path, and speeds were within one mile per hour of the target speed.

3.3 Test Speed

The aim of this work was to produce a ball deformation that is representative of play conditions. To determine the test speed, an impact speed with a rigid plate was needed that matched an impact with the recoiling cricket bat. Consider an energy balance

for an impact between a freely moving cricket bat (rotating mass) and a moving cricket ball (point mass).

The relationship between the cricket ball speed and the swing speed of cricket bat can be found by considering the impact speed between a cricket ball and rigid blocks with different masses m_1 and m_2 . The cricket ball impacts the stationary blocks 1 and 2 with an initial velocity of V_1 and V_2 , respectively. Let m_b be the mass of cricket ball with stiffness k . Both the cricket ball and block move with same speed, v at the point of maximum displacement, x_p , The energy balance is then

$$\frac{1}{2}m_p V_i^2 = \frac{1}{2}kx_i^2 + \frac{1}{2}(m_b + m_i)v_i^2 \quad (3.1)$$

where $i= 1$ or 2 for collision between the cricket ball and block 1 and 2, respectively.

Momentum is conserved during the impact according to

$$m_b V_i = (m_b + m_i)v_i \quad (3.2)$$

Equation (3.1) and (3.2) may be combined to eliminate v_i as

$$m_b V_i^2 = kx_p^2 + \frac{m_b^2 V_i^2}{(m_b + m_i)} \quad (3.3)$$

If the impacts with block1 and 2 are identical the ball displacement should be the same for each case. By evaluating Eq. 3.3 for block 1 and 2, x_p may be eliminated to produce

$$V_1 = V_2 \left(\frac{1 + \frac{m_p}{m_1}}{1 + \frac{m_p}{m_2}} \right)^{1/2} \quad (3.4)$$

For the case when the block 1 is infinitely large, m_1 becomes infinity, so m_p/m_1 approaches zero.

For the scenario of swinging object, m_2 becomes the swing-weight or I/b^2 where I is the moment of inertia and b is the distance between the impact location and the pivot point. Substituting Eq. (3.1) into Eq. (3.4) results in

$$v_2 = v_1(1 + r_i)^{1/2} \quad (3.5)$$

where v_2 and v_1 are the incoming ball speeds in the rigid wall tests and play, respectively. The bat recoil factor, r_i is defined as

$$r_i = \frac{m_b b^2}{I_i} \quad (3.6)$$

where m_b is the mass of the cricket ball, b is the distance between the impact location and the pivot point of the cricket bat, and I is the mass moment of inertia of the bat with respect to the pivot point [3.7]. Using a cricket bat pivot distance of 22 inches with 9800 oz.in² mass moment of inertia, a bat-ball relative speed of 60mph and cricket ball of 5.65 oz, the rigid wall ball speed is 53 mph.

3.4 Dynamic Properties

The performance of the cricket ball can be compared by its coefficient of restitution (e), (ASTM 1887 [3.5]). The ball was impacted on four sides: two faces and two seams. The ball was rotated 90° after every impact so that each face and seam of the ball was impacted one in four times. The coefficient of restitution (e) was measured as the ratio of the rebound and inbound speeds, as

$$e = \frac{-v_2}{V_1} \quad (3.7)$$

where V_1 and v_2 are the inbound and rebound speeds of the cricket ball, respectively. For a typical bat, a 2.0% increase in the COR can raise bat performance 1% [3.6].

The hysteresis from loading and unloading of the cricket ball can be described from the force vs. displacement curve. Displacement was obtained by dividing the force by the ball mass and integrating it twice, since

$$\frac{d^2x}{dt^2} = \frac{F}{m_b} \quad (3.8)$$

where F is the force (lb), m_b is the mass of the ball and with the initial conditions $x = 0$ at time $t = 0$ and $dx/dt = V_i$ at time $t = 0$. Fig. 3.7 shows a sample hysteresis plot for a cricket ball impacting a flat plate at 70mph.

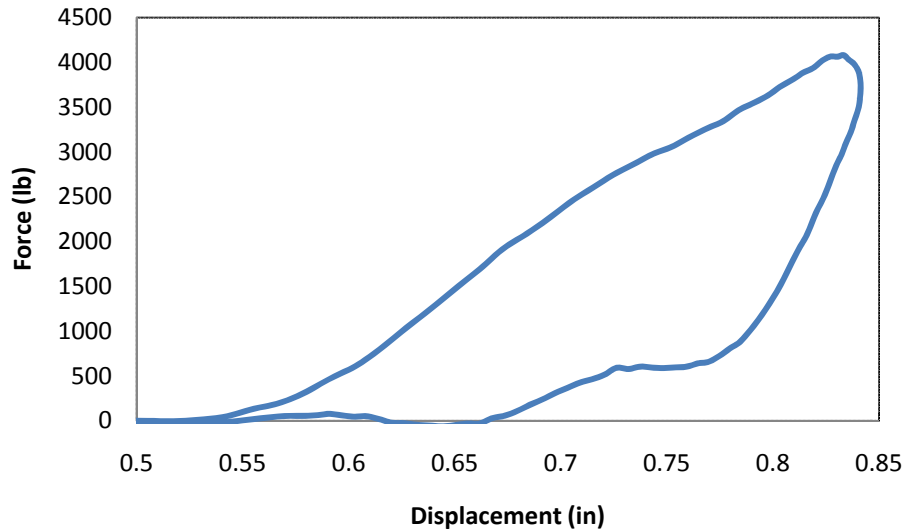


Figure 3.7: Hysteresis plot of cricket ball impacting at 70mph.

3.5 COR and Dynamics Stiffness Results

In the current study, balls from two different manufactures were used (Ba and Bb) Fig. 3.8. These balls are regularly used in the First-class cricket in different countries. The coefficient of restitution, (COR) and dynamic stiffness of six balls of each Ba and Bb were tested at 53mph. The cricket balls were impacted six times, from which the average COR and dynamic stiffness was obtained. Fig. 3.9 shows the difference in average COR and average dynamic stiffness for Ba and Bb. On average, the dynamic stiffness of ball models Ba was 19% higher than Bb. The average COR values were closer than the dynamic stiffness, where model Ba was 5% higher than Bb.

The difference in dynamic properties may be due to the difference in the construction of the cricket balls. Ball model Bb has a uniform construction with a modeled rubber core where model Ba has a cork core which was only approximately spherical. The different ball construction and materials likely contribute to their

characteristic response. In the following, the error bars represent the standard deviation for each case. The standard deviation of dynamic stiffness was nearly twice that for COR.



Figure 3.8: Cross sectional view of cricket ball Ba and Bb.

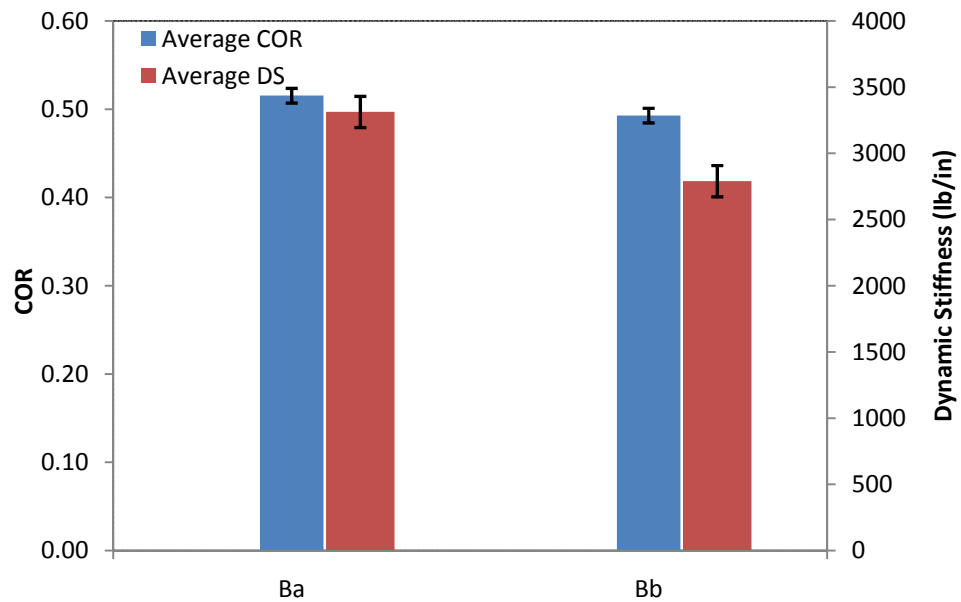


Figure 3.9: The average COR and dynamic stiffness of model Ba and model Bb.

Cricket balls have a pronounced seam that may produce a different response than the face. To consider this difference, seam and face impacts were compared between balls Ba and Bb as shown in Fig. 3.10. The average dynamic stiffness for Ba and Bb at the seam was 3% higher than the face. The average COR at the seam was 2% higher than the face. It is thought that the increased stiffness in the seam impact is due to the presence of the seam itself rather than the construction of the balls. Previous results for stiffness and hysteresis loss was found from drop test range around 13mph and quasi-static tests, which is much lower than the test speed used in this study [2.18]. The results here indicates different trend which may be the test used previously doesn't correspond to the actual play conditions.

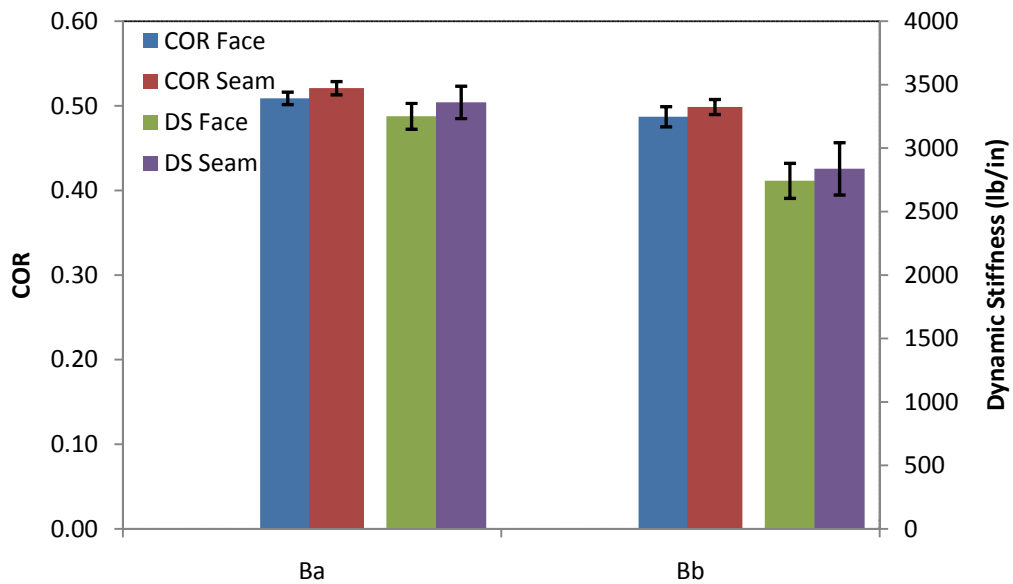


Figure 3.10: Comparison between the dynamic properties of Ba and Bb.

3.6 Rate Dependence

It is important to understand the behavior of the cricket ball under various impact speeds. Previous studies have shown that the softball and baseball COR decreases linearly with increasing impact speed [3.7].

In the current study 20 balls, of Ba and Bb were used. The balls were impacted at speeds ranging from 60mph to 80mph. Each ball was impacted six times; three times on the seam and three times on the face at each impact speed. Fig. 3.11 shows the average COR and DS as a function of speed. The COR decreased linearly with increasing impact speed. The increasing DS as a function of speed shows that cricket ball behaves as non-linear spring. The DS had a higher variation than COR as shown previously in Fig. 3.10.

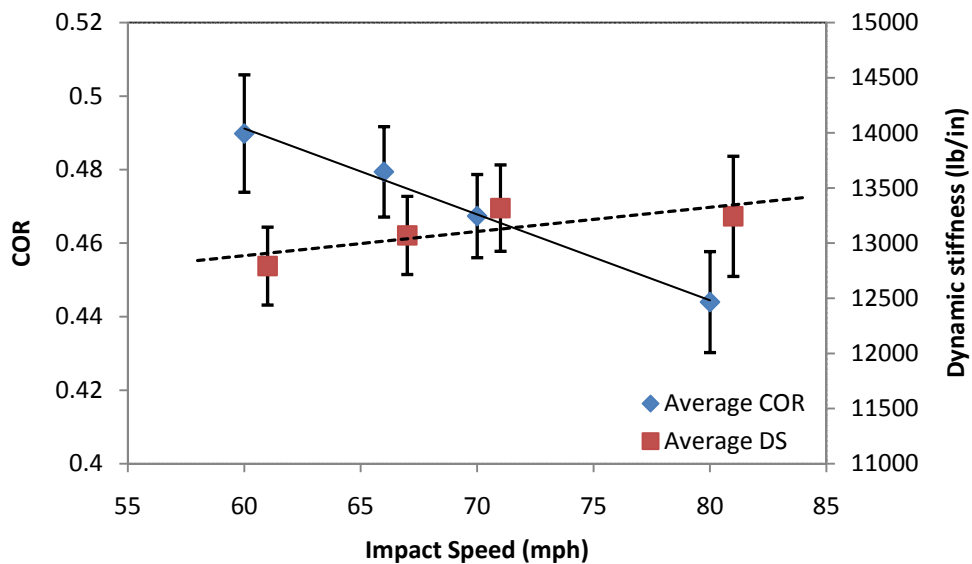


Figure 3.11: Average COR and DS as a function of increasing speed.

The DS in Fig. 3.11 was found for a linear spring. A nonlinear spring may be considered using Eq. 2.15. To determine the degree of nonlinearity, the exponent n was

varied until the stiffness was constant with the speed. Ball model Ba was used for this study, where k was constant with $n=1.27$ (Fig 3.12). This response is similar to softball ($n=1.25$) and classical Hertzian contact ($n=1.5$).

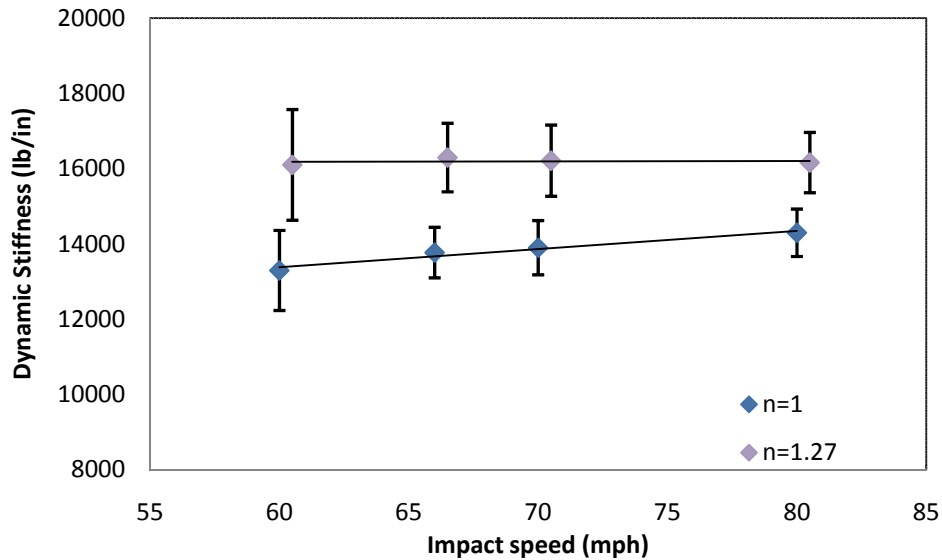


Figure 3.12: Linear and non-linear stiffness of the cricket ball impact at different speeds.

The effect of speed on COR of each ball model are compared in Fig. 3.13. It was found that the difference in COR between the models increased with speed. The different speed dependence of the ball models suggests that different ball models have a different rate-dependence, which further may be related to the construction of each ball model.

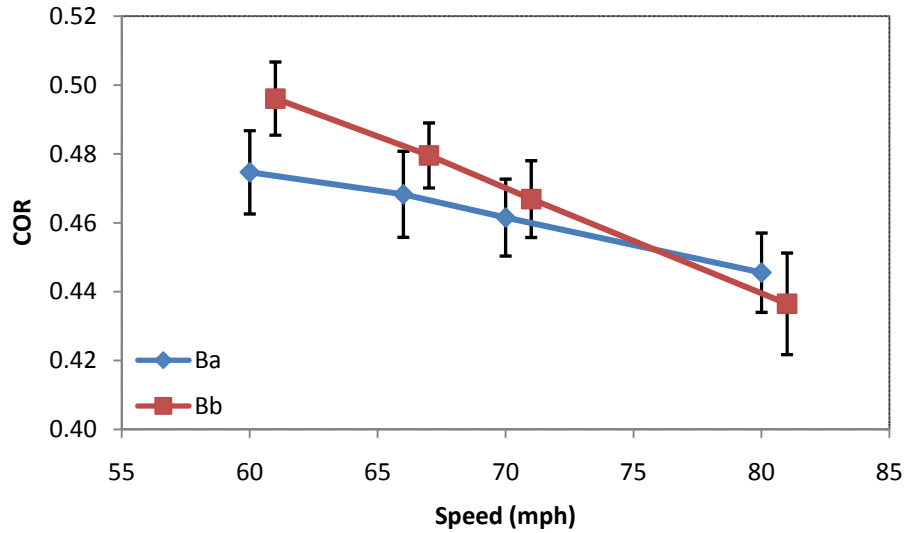


Figure 3.13: Comparison of COR for Ba and Bb models (6 balls at each point).

The dynamic properties of ball can be considered with force-displacement curves. The force vs. displacement curve for seam and face impacts is plotted for both models as a function of increasing impact speed in Fig. 3.14-3.17.

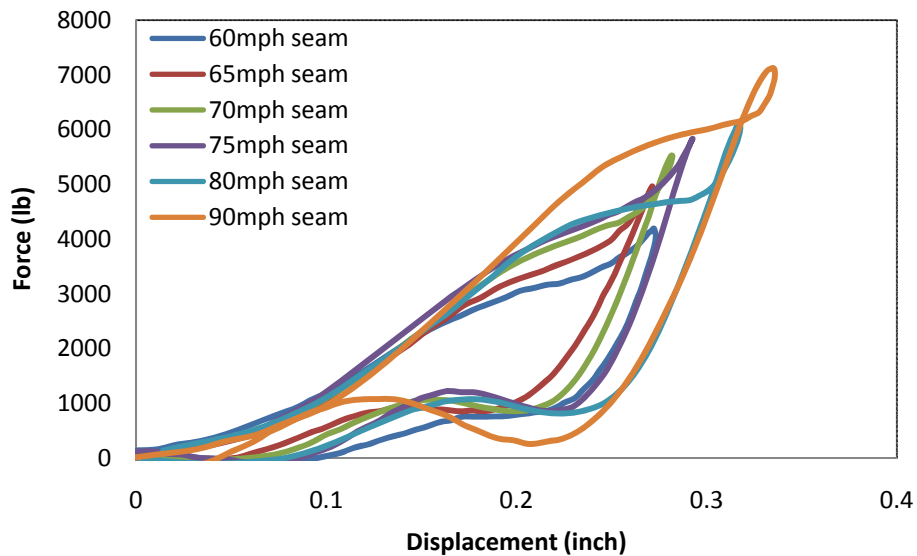


Figure 3.14: Representative force-displacement curves for Ba seam impacts.

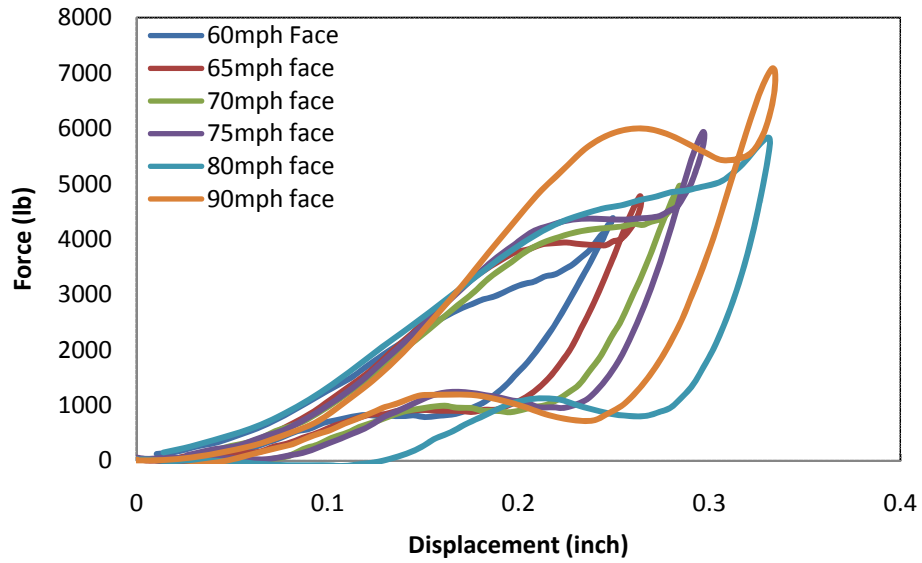


Figure 3.15: Representative force-displacement curves for Ba face impacts.

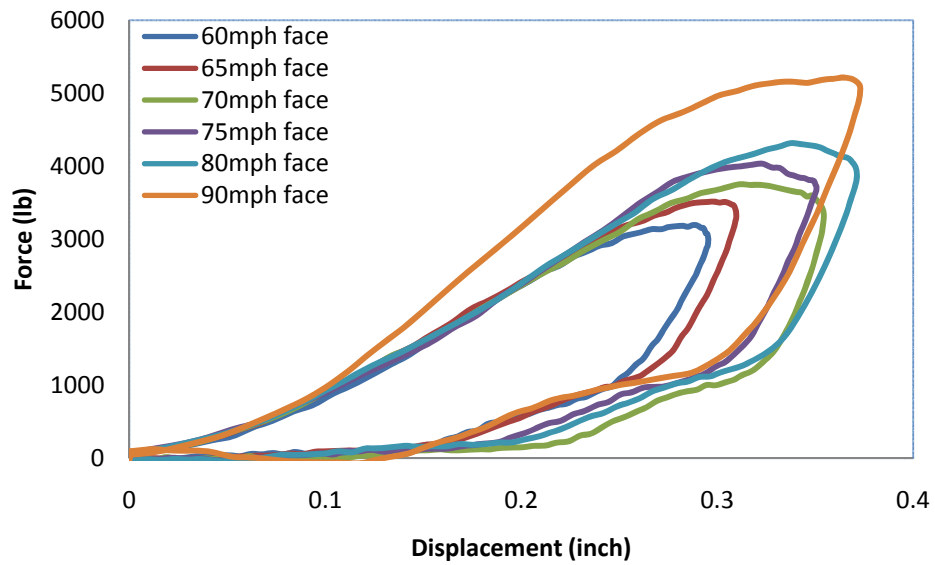


Figure 3.16: Force-displacement curve for Bb face impacts.

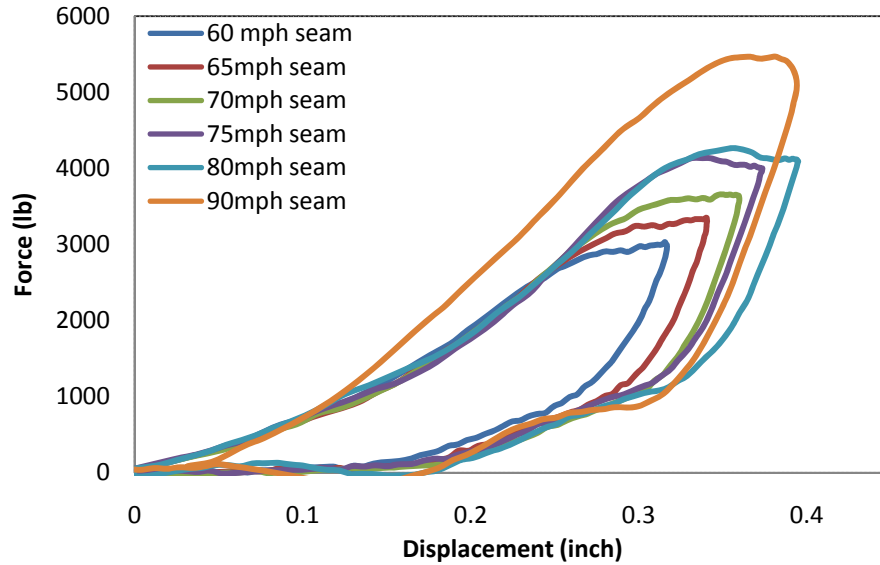


Figure 3.17: Force-displacement curve for Bb seam impacts.

On average, Bb had 17% more deformation than Ba when impacted at 90 mph. The hysteresis of Ba shows a characteristic loop at the maximum force. The force displacement difference is likely due to the difference in the construction of models, where model Ba has a cork core. The construction of Bb was more uniform than Ba, which may have affected the repeatability. The standard deviation of the COR and dynamic stiffness was 56% and 35% higher, respectively, for Ba, for instance. The uniformity of model Bb may have been achieved by its molded rubber core. The solid cork core of ball Ba was only approximately spherical.

3.7 Static compression

Method ASTM F1888 was used to characterize the hardness of cricket balls [3.8]. The cricket ball was placed between the two plates, and a preload of 4 ± 1 pounds was applied. The cricket ball was compressed $\frac{1}{4}$ " over a 15 second time period and the maximum force was recorded. The cricket ball was rotated 90° and the ball was

compressed again. Figure 3.20 and 3.21 shows the fixture for both seam compression and face compression. The average of two peak forces was taken as the static compression.

The average static compression of 33 balls of Ba and Bb was measured. Fig. 3.18 represents the static compression and dynamic stiffness of the cricket balls. The compression of model Ba was 135% higher than Bb. The difference decreased for dynamic stiffness measured at 60mph, where Ba was 37% stiffer than Bb. Fig. 3.19 shows the comparison between the face and seam static compression of ball models Ba and Bb. It can be seen that, on average face static compression is 16% higher than seam static compression. The study done previously [2.18] on the face and seam compression shows opposite results from this study. In this study, both the dynamic stiffness and static compression shows the same end results. In this study dynamic stiffness, the impact speed used is representative of the playing conditions, whereas the impact speed of the previous study was much lower.

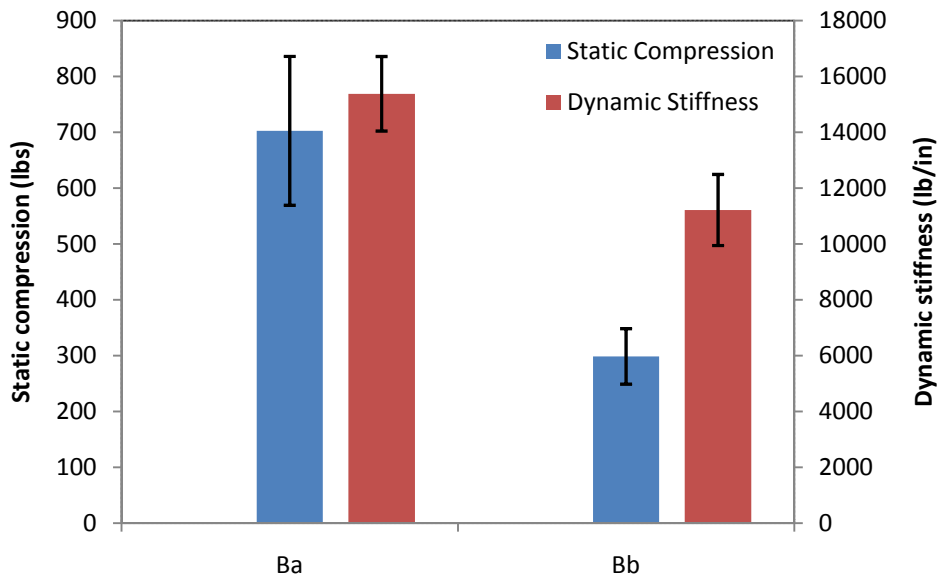


Figure 3.18: Static and dynamic stiffness of cricket balls.

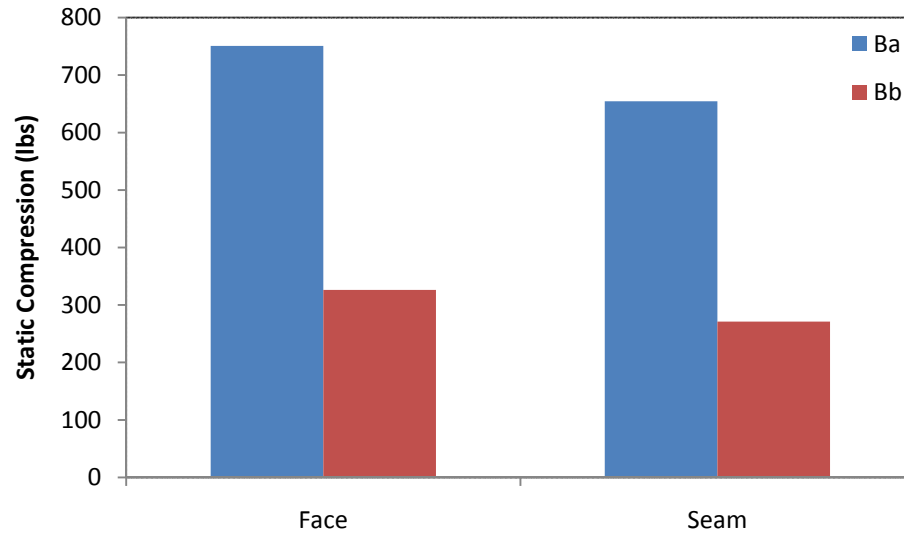


Figure 3.19: Face and seam static compression of ball model Ba and Bb.



Figure 3.20: Seam Compression of the cricket ball.



Figure 3.21: Face compression of the cricket ball.

3.8 Summary

The goal of this study was to evaluate the COR and dynamic stiffness of various cricket balls. The results show that the COR of all the balls decrease with increasing impact speed. The dependence of COR on speed appeared to be related to the ball construction.

Seam impacts had higher COR and higher dynamic stiffness than a face impacts. The dynamic stiffness increased with speed using a linear spring model. A gradual increase in displacement and force with the impact speed was observed. The peak displacement shows linear relationship with impact speed. The relationship between peak force as a function of impact speed is non-linear. This may be due to the construction of the cricket ball models. Results reveal that the ball Ba which contains rubber core have

lower COR than ball Bb with cork core. It suggests that the different ball construction most likely contribute to their dynamic response.

REFERENCES

- [3.1] The laws of Cricket – 2000 Code, Marylebone Cricket Club, London, 2000
- [3.2] Tom P., Daryl F. and Brain B. “Release Velocities of fast bowlers during a cricket test match” Supplement to the Australian Journal for Health, Physical Education and Recreation. March 1976
- [3.3] Carre, M.J., James, D.M., Haake, S.J. “Impact of a non-homogeneous sphere on a rigid surface”. Proceeding of the institution of Mechanical Engineers, Journal of Mechanical Engineering science. Vol. 218 Part C: pp. 273. 2004
- [3.4] Nathan, A. M. “Characterizing the Performance of Baseball Bats” Am. J. Phys, 71 (2). February 2003
- [3.5] ASTM F 1887 Standard Test Method for Measuring the Coefficient of Restitution (COR) of Baseball and Softballs, ASTM International 2004.
- [3.6] Adair, R.K. *The physics of baseball*. New York, Harper and Row, 3rd edition. 2002.
- [3.7] Chauvin, D.J., Carlson, L.E. *A comparative test method for dynamic response of baseballs and softballs*. International Symposium on Safety in Baseball/Softball. ASTM STP 1313, p. 38-46. 1997.
- [3.8] Nathan, A. M. 2003. Characterizing the Performance of Baseball Bats, American Journal of Physics, 71.2:134-143.
- [3.7] Smith, L. V. Measuring the Hardness of Softballs, Abstract Proc. of the Society for Experimental Mechanics, Spring Conference, Orlando, Florida, 2008
- [3.8] ASTM F1888-04 Standard Test Method for Compression-Displacement of Baseballs and Softballs, ASTM International, Pennsylvania (2004).

CHAPTER 4

-BAT TESTING-

4.1 Introduction

The aim of the bat is to send the ball to its home by playing the most powerful shot, and minimizing shock to the batsman's hand. The blade is commonly made of English or Kashmir willow which is strong, lightweight and has good shock resistance. The handle is made of cane which has good shock absorbing properties. As shown in Fig. 4.1 the length of the bat cannot exceed 38 inches (96.5 cm) and the width of the blade must be less than 4.25 inches (10.8 cm) [4.2]. A material can be used to protect, repair or strengthen the blade of the bat; but must be limited to 1/16 inches (1.56mm) in thickness and may not cause any harmful damage to the ball. There is no law covering the weight of the cricket bat [4.2].

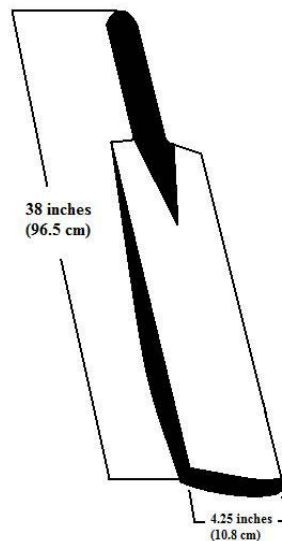


Figure 4.1: Dimensions of Cricket bat according to Law 6 [4.2].

During the manufacture of a bat, the blade is compressed (knocked) in order to resist the dynamic impact of the ball without getting damaged. Little has been done, however, to consider the effect of knock-in or wood species on performance. Studies have shown that the surface hardness of the cricket bat increases with knocking, which produces a stiff and dense region that affects the flexural stiffness and vibration of the bat [4.3], [4.4]. Recent advances in technology and materials have motivated a number of changes in cricket bat design. Advanced composite materials are used to stiffen the blade and is purported to improve durability. While some studies suggest these advances have not affected performance, more work is needed to quantify their contribution [4.5].

The current study compares the effect of surface hardness, wood species and composite reinforcement on the performance of the cricket bats. An experimental test apparatus was developed to measure the performance of cricket bats under dynamic impact conditions representative of play. A bat performance measure was derived in terms of an ideal batted-ball speed based on play conditions.

The performance of five cricket bats with different structural, geometrical and material properties was measured. Bats manufactured from Kashmir willow, English willow and with a composite skin were compared. The bats were identified by a code, where the first character indicated the material (K=Kashmir, E=English willow), the second letter was the sequential number of the cricket bat, followed by the third letter for knock-in or unknock-in (Knock-in=K, Unknocked=U). As there was only one composite bat the code for the cricket bat with and without a composite skin was CS and CWS respectively. For example E2U means the bat material is English willow, it is 2nd bat in the order and it is unknocked.

4.2 Experimental Apparatus setup

4.2.1 MOI Apparatus

The swing speed of the bat depends upon the swing-weight, which is described by the MOI of the bat [4.6]. The MOI of the cricket bat was determined by ASTM F2398-04 (used to measure the MOI of the baseball and softball bats) [4.7]. The MOI of the cricket bat was measured as a physical pendulum, rotating about a pivot 6 inches from the end of the handle [4.8]. The apparatus used to measure the moment of inertia of the cricket bat is shown in the Fig. 4.2. The bat was placed on the MOI apparatus so that the bat could swing freely on the clamp pivot points. The average of five repeatable readings with 10 oscillations for each reading was used to measure the MOI of the cricket bat. The acceptable average standard deviation of each reading was 0.0005sec.



Figure 4.2: Experimental apparatus used to measure the MOI of the cricket bat.

The MOI was measured to the nearest 1oz-in² using:

$$I = \frac{T^2 mgd}{4\pi^2} \quad (4.1)$$

where I is the moment of inertia, m is the mass of the cricket bat, T is the oscillation time period, g is the gravitational constant, and d is the distance from the pivot point to the balance point. The balance point (BP) was determined by

$$BP = \frac{(6W_6 + 24W_{24})}{W_6 + W_{24}} \quad (4.2)$$

where W₆ was weight at 6 inches and W₂₄ was weight at 24 inches, from the knob end of the bat. The MOI, length and weight of the cricket bats are listed in Table 4.1.

Table 4.1: Properties of different cricket bats

Bat code	Length (in)	Weight (oz)	MOI (oz-in ²)
K1U	33.6	41.2	11227
K1K	33.6	41.3	11258
K2U	33.8	40.4	11638
K2K	33.8	40.5	11617
K3U	33.5	39.2	10630
K4U	33.7	40.4	11340
K5U	33.6	39.9	10839
K6U	33.9	40.5	11128
E1U	33.4	37.7	9799
E1K	33.4	37.5	9774
E2U	34.9	39.5	11779
E2K	34.9	39.5	11801
E3U	33.8	38.6	10620
CS1	33.8	38.1	10703
CWS1	33.8	36.8	10266
CS2	34.5	37.0	10880
CWS2	34.5	36.2	10657

4.2.2 Bat Testing Equipment

The bat was tested using the fixture similar to the ball test as shown in Fig. 4.3, where the rigid wall was replaced by a pivot assembly as shown in Fig. 4.4. The pivot assembly allowed the bat to recoil after impact and controlled the impact location. Three pairs of ADC iBeam light gates were used to measure the inbound and rebound speed of the cricket ball. LabVIEW version 7.1 was used to record and reduce the data and control the impact location of the cricket bat on the pivot assembly.

In the bat tests an incoming ball speed of 60 mph was used to prevent accumulated bat damage from influencing the results. Each bat was impacted at $\frac{1}{2}$ inch increments to find the location with maximum performance. An average value from six balls impacting the blade of the bat was used to determine the maximum performance. The ball was rotated along the common axis so that face and seam impacts occurred at each location.



Figure 4.3: Experimental test fixture used to test cricket bats.

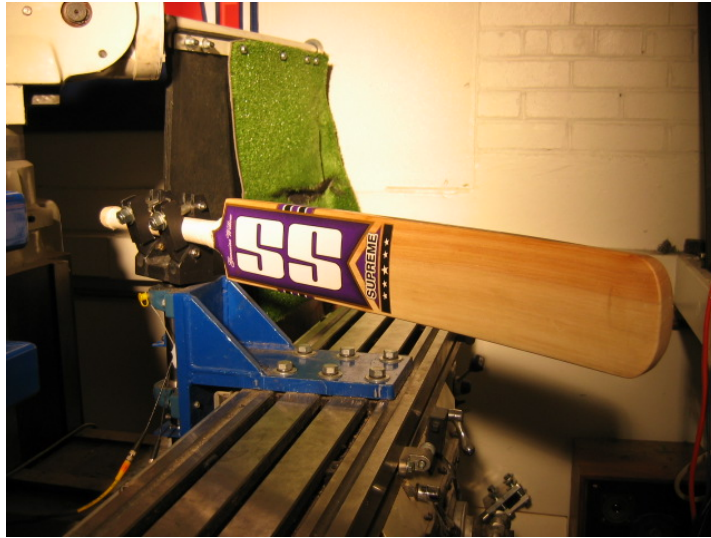


Figure 4.4: Pivot assembly used to test cricket bats.

4.3 Bat Performance Metric

Light gates measured the ball speed before and after impact. The ratio of the rebound to inbound ball speed is the so-called collision efficiency, e_a [4.9]

$$e_a = \frac{-v_2}{V_1} \quad (4.3)$$

where v_2 and V_1 are the ball speeds after and before impact, respectively. The negative sign indicates that the cricket ball travels in the reverse direction after impact with bat. If the bat speed, v_b , and ball speed, v_p , in play conditions are known, the collision efficiency may be used to find the batted ball speed, BBS in play, according to

$$BBS = e_a v_p + (1 + e_a) v_b \quad (4.4)$$

The bowled ball speed is relatively easy to measure in play and is usually taken as a constant when comparing bat performance. In this work it was taken as 85 mph.

The bat speed is more difficult to measure and has a greater effect on the BBS. Bat swing speed depends upon the mass properties of the cricket bat. The bat swing consists of both rotational and translational motion in three-dimensional space. For this work the bat was assumed to pivot about a point 6 inches in from the knob. The following was used to account for the effect of MOI on swing speed

$$v_b = v_s \left(\frac{Q}{21} \right) \left(\frac{10,000}{MOI} \right)^{1/4} \quad (4.5)$$

where v_s is the nominal bat swing speed (21 inches from the pivot), MOI is the moment of inertia and Q is impact location (both taken from the pivot position). The nominal bat swing speed was found by considering a ball flight trajectory of 250 feet. The distance traveled by the cricket ball was found from its BBS, spin, and launch angle. The launch angle was assumed to be 35 degrees from the horizontal as balls launched at 30-40 degree travel the maximum distance [4.15].

The spin of the ball affects its distance. Backspin causes the ball to stay in the air longer and allows the ball to travel further, whereas forward spin decreases the distance. For this study a 500rpm back spin was used. The Magnus force was found according to [4.15]

$$F_m = KfVC_d \left[1 + 0.5 \left(\frac{dC_d / C_d}{dV / V} \right) \right] \quad (4.6)$$

where f was spin frequency in rpm, V is velocity of the ball in mph, C_d is drag coefficient and $K \approx 2 \cdot 10^{-6}$. The drag force can be written as [4.15]

$$F_d = C_d A \rho \frac{V^2}{2} \quad (4.7)$$

where $A = \pi r^2$, with r the radius of the ball, ρ is the air density, V is the BBS of the ball.

The drag coefficient is not constant but is a function of speed as shown in Fig. 4.5. [4.18].

In a standard cricket arena the home fence varies from 225 feet to 250 feet from the batter. Fig.4.6 shows an example of ball with an initial BBS of 70mph, launch angle of 35 degree and spin of 500rpm. Fig. 4.7 shows the distance traveled by a ball at different velocities. For a ball to travel 250 feet, a BBS of 80 mph is needed. Solving Eq. 4.4 for v_b with $e_a = 0.25$ (representative of cricket bats), $v_p = 85$ mph and BBS = 80 mph produces a nominal bat speed of $v_s = 47$ mph.

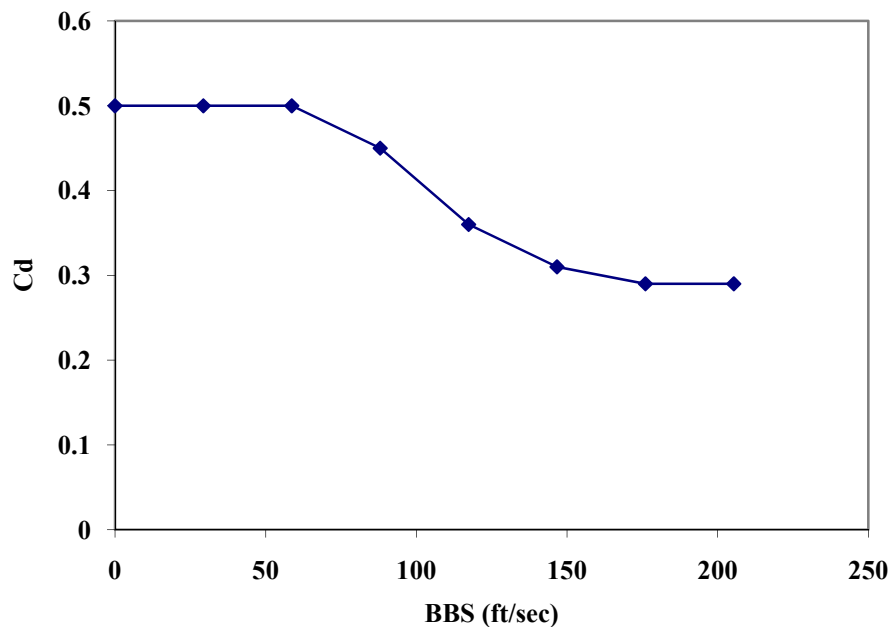


Figure 4.5: Drag coefficient vs. BBS of the cricket ball.

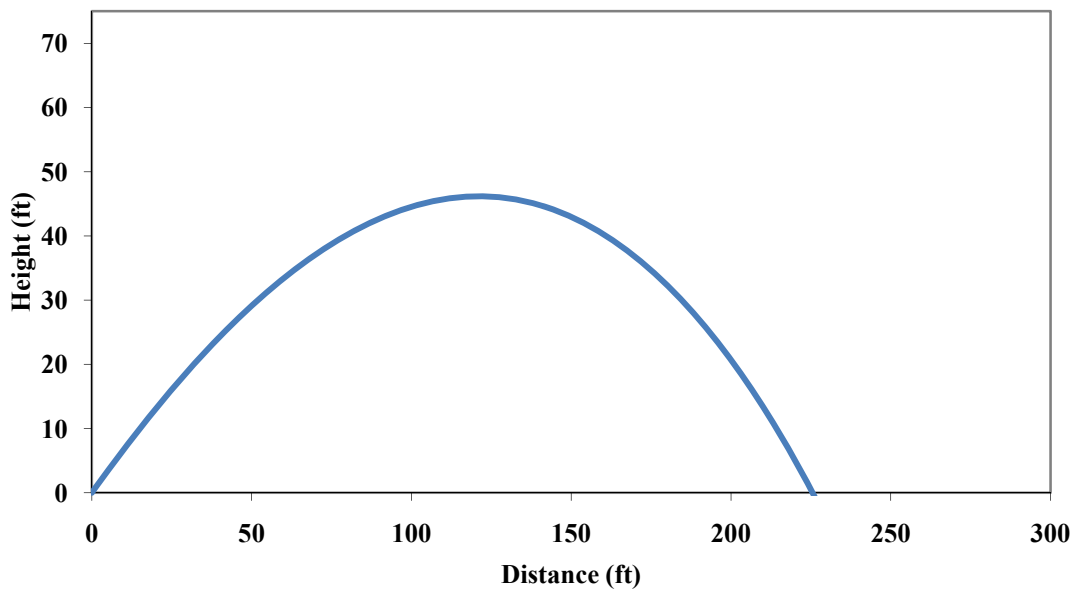


Figure 4.6: Maximum distance travelled by the ball launched at 35 degree with 500rpm and with velocity of 70mph.

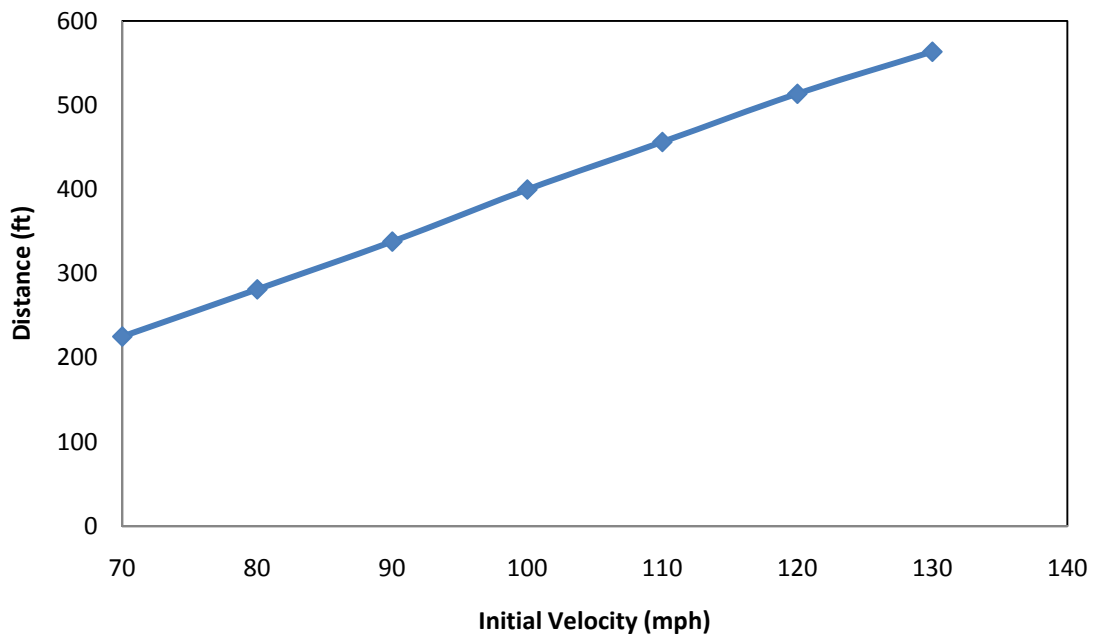


Figure 4.7: Comparison between the initial velocity and the distance travelled by a cricket ball.

4.4 Test Results

Each bat was impacted six times at multiple locations along its length until a maximum BBS location was found within 0.50 inches. A representative bat performance curve is shown in Fig. 4.8. Note the relatively small region which produces an optimum BBS.

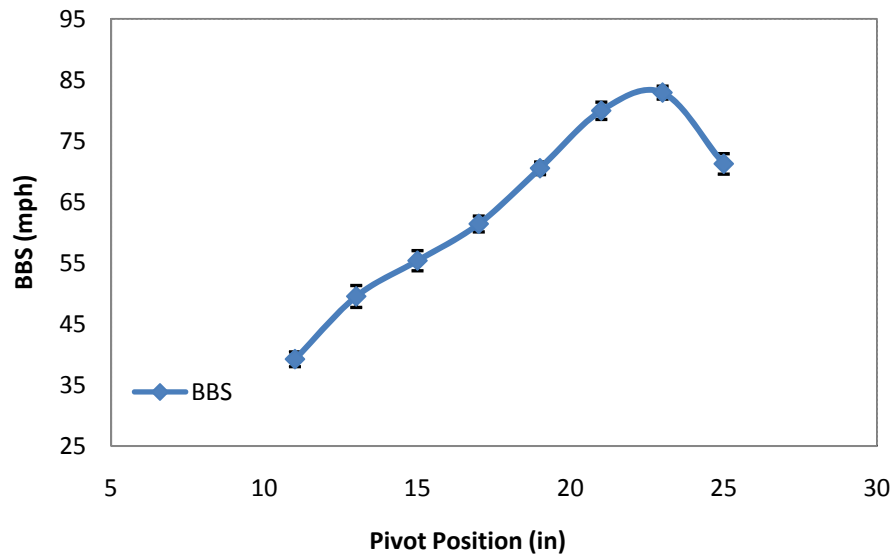


Figure 4.8: Bat performance curve of E2.

4.4.1 Knock-in/oiled

A variety of treatments are applied to bats and incorporated in their design to improve their performance. Many believe that due to the soft and fibrous nature of the wood fibres, knock-in and oil treatment should be done to the bat before play. Knock-in is the process of squeezing the fibres on the surface of the cricket bat by hitting the surface with a wooden mallet or with an old ball for 2-4 hours [4.12]. The surface of the blade is commonly knocked-in and oiled to make the bat more durable. To consider the effect of knock-in on performance, the bats (except CS1, CS2, CSW1 and CWS2) listed

in Table 4.1 were tested before and after knock-in. The process was performed by hitting the surface of the cricket bat with a wooden mallet for 2 hours which was separated in 12 sessions of 10 minutes each.

The average BBS of the cricket bat before and after knock-in and oiling is shown in Fig. 4.9. The maximum average BBS for the knocked bats was 0.2 mph lower than the unknocked bats. Knock-in was observed to have a relatively small effect on performance, decreasing it by 0.03%. Interestingly many believe that knock-in increases the stiffness which further increases the performance of the cricket bat.

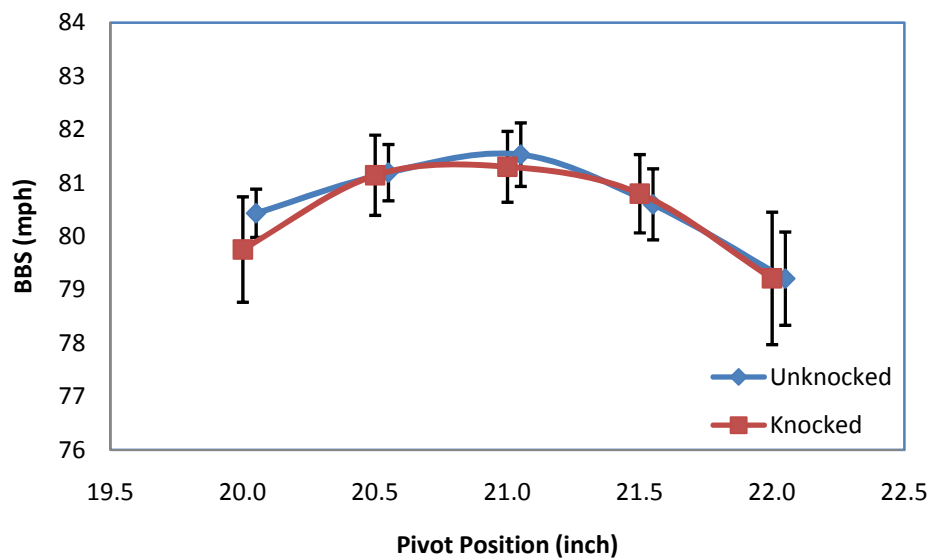


Figure 4.9: Average performance between knocked and unknocked bats.

It was interesting to compare the knock-in and oiled effect on the cricket bats individually. For Bat E1 the peak BBS reduced by 1.97% after knock-in and oiling. Bat E2 showed an increase of 2% in the peak BBS after knock-in and oiling.

4.4.2 Material Comparison

The blade of most cricket bats is made of either Kashmir or English willow. Many view English willow as superior, for which a premium price is usually paid. The average performance of two English (E1 and E2) and Kashmir willow (K1 and K2) bats are compared in Fig. 4.10, where the performance of English willow was observed to be 0.02% higher than Kashmir willow. There was a shift in the peak location in English willow after knock-in.

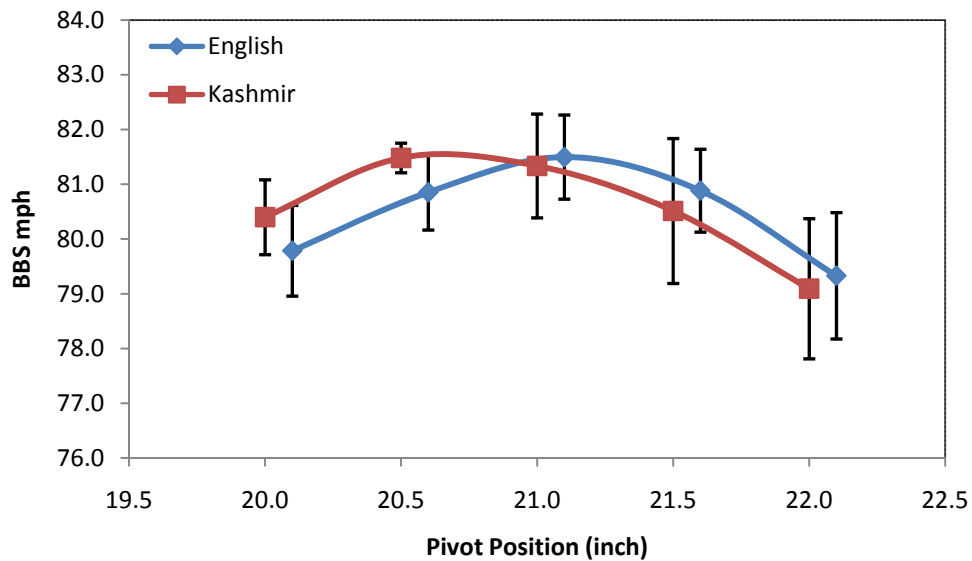


Figure 4.10: Average performance between English willow and Kashmir willow after knock-in and oiling.

The effect of weight on the performance can be observed by comparing the MOI and BBS of the different cricket bats. Fig. 4.11 shows the BBS as a function of bat MOI for English and Kashmir willow bats. It was observed that BBS increased with increasing MOI of the bats. Both unknocked and knocked bats are included in this study.

Bat performance should increase with flexural stiffness. A three point bend test was performed on 12 cricket bats as shown in Fig.4.12. A span of 24 inches was used to deflect the cricket bats 0.2 in in a load frame (MTS Systems Corporation, MN). Force was applied and displacement was measured at 11 inches from the toe end of the bat. Figure 4.13 compares the average bat stiffness for each material. Interestingly the Kashmir willow was stiffer than the English willow and composite reinforced bats.

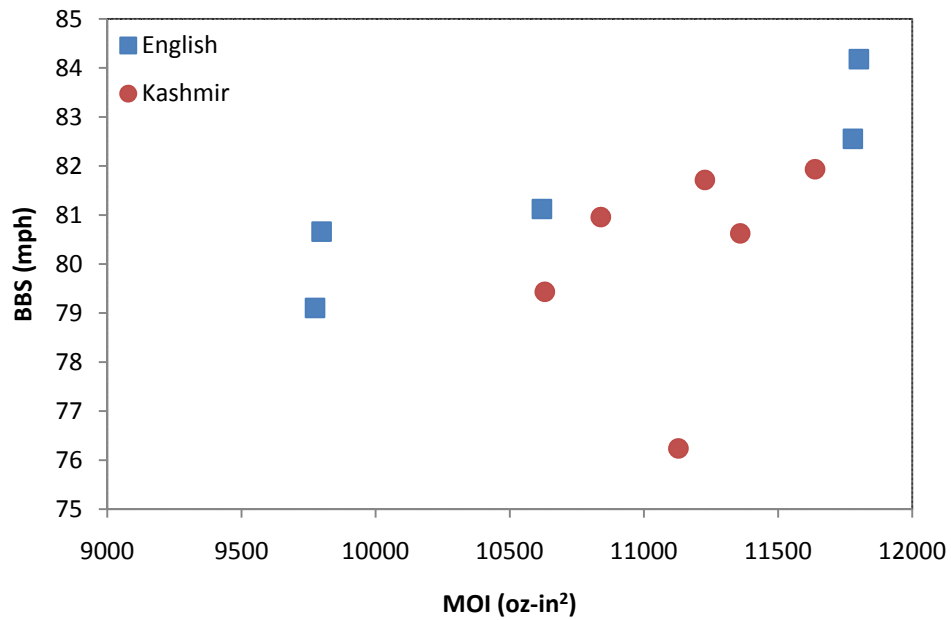


Figure 4.11: BBS as a function of MOI for English and Kashmir willow bats.



Figure 4.12: Cricket bat bending stiffness test.

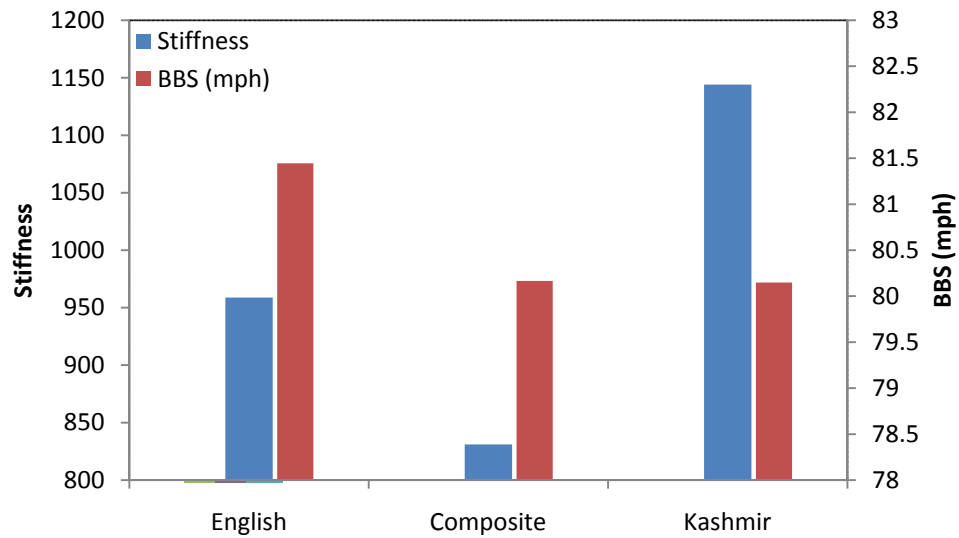


Figure 4.13: Average stiffness results from 3-point bend tests.

The composite skin stiffens the blade and is purported to improve durability. The performance of bats was compared with and without a composite skin. The results are included in Fig. 4.14, which shows the skin increased the BBS by 1.44%. It should be noted that removing the skin reduced the bat’s MOI by 4.6%. It is helpful to consider

how much of the composite skin performance was due to its added MOI. BBCOR is insensitive to MOI and is given as,

$$e_{BB} = \frac{v}{V} + \frac{mQ^2}{VI_p}(V + v) \quad (4.8)$$

where V , m , v , and I_p are inbound ball speed, weight, rebound ball speed and moment of inertia, respectively. The collision efficiency is found from e_{bb} as

$$e_a = \left(\frac{e_{BB} - r}{1 + r} \right) \quad (4.9)$$

where r is the bat recoil factor (Eq. 3.6). The effect of MOI on bat performance, independent of the composite skin, may be considered in Eq. (4.4) by holding the bat-ball COR constant and changing the bat MOI. Accordingly, a 4.5% change in MOI was found to increase bat performance by 0.92%. Thus, roughly half of the performance advantage attributed to a composite reinforced blade is due to its mass.

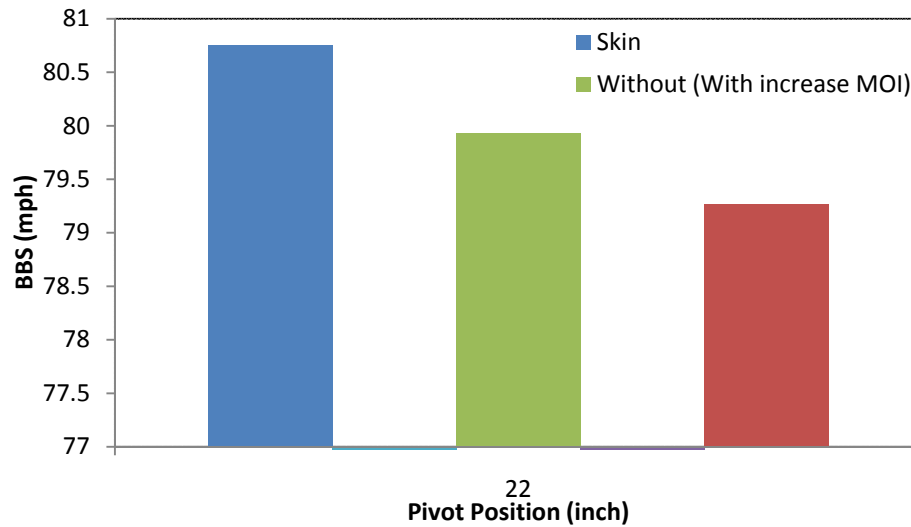


Figure 4.14: Comparison of cricket bat with and without composite skin.

4.5 Summary

This study considered the performance of cricket bats. A test apparatus was developed to measure bat properties at impact speeds representative of the play conditions. The test method involved firing the cricket balls at various positions on a stationary cricket bat. Bat performance has been compared using the BBS of cricket bats. The swing speed of the cricket bat was found from the flight of the cricket ball. The MOI of the cricket bat has a significant effect on the performance. Knock-in and oiling has a small effect on weight, MOI and performance.

On average, the performance of English willow was observed to be 0.8% higher than Kashmir willow. The contribution of a reinforcing composite skin to the back surface of the bat was also relatively small (1.4%), although larger than the effect of knock-in or willow species. It should be noted, however, that one half of this advantage was due to the weight of the composite.

References:

- [4.1] Bowen, R “Cricket: a history of its growth and development throughout the world” London, Eyre and Spottiswoode, 1970.
- [4.2] The laws of Cricket – 2000 Code, Marylebone Cricket Club, London, 2000
- [4.3] Sayers, A. T., Koumbarakis, M., Sobey, S. “Surface Hardness of a Cricket Bat after ‘Knock-in’”. Sports Engineering, p233-240, 2005
- [4.4] Grant, C. and Nixon, S.A. “The Effect of Microstructure on the Impact Dynamics of a Cricket Bat, Proceedings of the International Conference on the Engineering of Sport, Sheffield U.K., In Haake S. (ed.), The Engineering of Sport, Balkema, Rotterdam, p169-173, July 1996
- [4.5] Stretch, R.A., Brink, A. and Hugo, J. “A Comparison of the Ball Rebound Characteristics of Wooden and Composite Cricket Bats at Three Approach Speeds”. Sports Biomechanics Vol. 4(1) pages 37-46, 2006
- [4.6] Smith, L., Broker, J., and Nathan, A. “A study of softball player swing speed”. In A. Subic, P. Travaglio, and F. Alam (Eds.), Sports dynamics: Discovery and application Melbourne, VIC: RIMT University pages 12-17 2003
- [4.7] ASTM F 2398-04, Standard Test Method for Measuring Moment of Inertia and Center of Percussion of a Baseball or Softball Bat, ASTM International 2004.
- [4.8] Russell, D. “Swing Weight of a Softball bat” Submitted to The Physics Teacher. Kettering University, Flint, MI, 2006
- [4.9] Carre, M. J., James, D. M. and Haake, S. J. “Impact of a Non-homogeneous Sphere on a Rigid Surface” Proceedings of the Institution of Mechanical Engineers; ProQuest Science Journals; 218, 3; p273, March 2004
- [4.10] Penrose, T., Foster, D. and Blanksby, B. “Release Velocities of Fast Bowlers During a Cricket Test Match” Supplement to the Australian Journal for Health, Physical Education and Recreation, p2-5, March 1976
- [4.11] Smith, L., Axtell, J., T. “Mechanical Testing of Baseball Bats” Journal of Testing and Evaluation; Vol. 31, No. 3, 2003
- [4.12] Sayers, A., T., Koumbarakis, M., Sobey, S. “Surface Hardness of a Cricket Bat After ‘Knock-in’ Sports Engineering, 8, pp 233-240; 2005

- [4.13] Smith, L. V., Cruz, C. M., Nathan, A. M., Russell, D. A. "How Bat Modifications Can Affect Their Response," APCST, Tokyo, Japan, The Impact of Technology on Sport, (Subic & Ujihashi, Eds) p. 33-38 2005
- [4.14] Cross, R. and Bower, R. "Effect of Swing-Weight on Swing Speed and Racket Power". Journal of Sports Sciences;24(1): p23-30, January 2006
- [4.15] Adair, R., K. "The Physic of Baseball" Third Edition, 2002

CHAPTER 5

-NUMERICAL MODEL-

5.1 Introduction

Sports such as baseball, softball, golf and tennis have benefited from research and technology, but the game of cricket has received relatively little attention. In this study finite element modeling was used to characterize the performance of cricket bats. Numerical models are valuable in providing a mathematical description of high-speed dynamic sport ball impacts [5.1].

The evaluation of cricket bat performance is nontrivial. Many factors affect the performance of the cricket bat, such as geometry of the bat, the properties of the ball, and the material properties of the wood. In the following study, the BBS was used to compare bat performance from finite element models.

5.2 Ball model

5.2.1 Numerical Analysis Background

All the simulations in this work were carried out using LS-DYNA (Livermore Software technology Corporation, Livermore, CA) Version 971. The cricket ball was modeled as a homogenous sphere with isotropic properties. The finite element analysis was carried out on a single 3.06Hz Intel Pentium 4 processor with 3 GB of RAM. Two bats of same the material with different geometry were considered. The effect of a composite skin on performance was also investigated.

A dynamic finite element simulation can be performed using either implicit or explicit time integration methods. Response is evaluated at instants separated by time increments Δt . At the n^{th} time step, the equation of motion can be written as [5.3], [5.9]

$$[M]\{\ddot{D}\}_n + [C]\{\dot{D}\}_n + [K]\{D\}_n = \{R\}_n \quad (5.1)$$

where $[M]$, $[C]$, $[K]$ and R_n are the mass, damping, stiffness matrix, and the known time-dependent forcing function at the n^{th} instant, respectively. An explicit method assumes a linear change in displacement over each time step. Once the displacement at t_{n+1} is determined, the velocity and acceleration at time step n are approximated by central the difference theorem as [5.3], [5.10]

$$\{\dot{D}\}_n = \frac{1}{2\Delta t}(\{D\}_{n+1} - \{D\}_{n-1}) \quad \text{and} \quad \{\ddot{D}\}_n = \frac{1}{2\Delta t}(\{D\}_{n+1} - 2\{D\}_n + \{D\}_{n-1}) \quad (5.2)$$

Equations 5.2 were be obtained from a Taylor series expansions for $\{D\}_{n+1}$ and $\{D\}_{n-1}$ at time $n\Delta t$ as

$$\{D\}_{n+1} = \{D\}_n + \Delta t\{\dot{D}\}_n + \frac{\Delta t^2}{2}\{\ddot{D}\}_n + \frac{\Delta t^3}{6}\{\ddot{\ddot{D}}\}_n + \dots \quad (5.2.a)$$

$$\{D\}_{n-1} = \{D\}_n + \Delta t\{\dot{D}\}_n + \frac{\Delta t^2}{2}\{\ddot{D}\}_n + \frac{\Delta t^3}{6}\{\ddot{\ddot{D}}\}_n + \dots \quad (5.2.b)$$

Subtracting Eq. (5.2b) from Eq. (5.2a) yields Eq. 5.2,. In both cases, the high order terms are discarded. Substitution of Eqs. (5.2) into Eq. 5.1 yields [5.10]

$$F(t) = R - \left[K - \frac{2}{(\Delta t)^2} M \right] D_n - \left[\frac{1}{(\Delta t)^2} M - \frac{1}{2\Delta} C \right] D_{n-1} \quad (5.2.c)$$

where, if linear conditions prevail, $F(t)=AD_{n+1}$. Thus for any n , D_{n+1} is calculated from values of D_n and D_{n-1} .

An implicit integration method assumes a constant average acceleration over each time step, between t_n and t_{n+1} . The equation of motion is evaluated and the resulting accelerations are used to obtain the velocities displacements at t_{n+1} as [5.3],

$$\{\dot{D}\}_{n+1} = \{\dot{D}\}_n + \Delta t[\gamma\{\ddot{D}\}_{n+1} + (1-\gamma)\{\ddot{D}\}_n] \quad (5.3.a)$$

$$\{D\}_{n+1} = \{D\}_n + \Delta t\{\dot{D}\}_n + \frac{1}{2}\Delta t^2[2\beta\{\ddot{D}\}_{n+1} + (1-2\beta)\{\ddot{D}\}_n] \quad (5.3.b)$$

where the numerical factors γ and β control the numerical accuracy, stability, and damping Substituting Eqs. 5.3.a and 5.3.b in Eq.5.1 we obtain

$$A = K + \frac{\gamma}{\beta\Delta t}C + \frac{1}{\beta(\Delta t)^2}M \quad (5.3.c)$$

$$F(t) = f(\beta, f, \Delta t, R, C, M, D_n, \dot{D}_n, \ddot{D}_n) \quad (5.3.d)$$

The complete expression is not written because it's lengthy and not essential to our discussion. Using Eqs. 5.3.c and 5.3.d, \ddot{D}_{n+1} is calculated from D_n , \dot{D}_n , and \ddot{D}_n .

An other difference between the two techniques is that in the explicit method the coefficient matrix of $\{D\}_{n+1}$ can be made diagonal, so that $\{D\}_{n+1}$ is cheaply inverted for each time step. In the implicit method, $\{D\}_{n+1}$ cannot be made diagonal, so that cost per step is greater [5.3]. Neither an implicit nor explicit solution is perfect in all cases. In the present study the implicit time integration method was used.

The cricket ball was represented as a solid isotropic sphere of radius 1.41 inches and 5.65oz. A viscoelastic material model (*MAT_006) consisting of 3584 eight node solid elements was selected for the cricket ball, defined by the time dependent shear modulus [5.2], [5.3], [5.4] as,

$$G(t) = G_{\infty} + (G_0 - G_{\infty})e^{(-\beta t)} \quad (5.4)$$

and a constant bulk modulus, k where G_0 is the instantaneous shear modulus G_{∞} is the long shear modulus, and β determines the time sensitivity of the model. The short term modulus is dominant near $t=0$, while near $t= \infty$ the long term modulus is dominant. The decay constant β determines the rate at which the long term modulus dominates the material response. The cricket ball can be tuned for COR and dynamic stiffness by adjusting one or more of the material properties.

Linear viscoelasticity was assumed for the deviatoric stress tensor, which was calculated from the Jaumann rate integral (also known as the hereditary integral) [5.5] as

$$\hat{\sigma}'_{ij} = 2 \int_0^t G(t-\tau) D'_{ij}(\tau) d\tau \quad (5.5)$$

where the prime denotes the deviatoric part of the stress rate, $\hat{\sigma}'_{ij}$, the strain rate D'_{ij} and τ is time. A recursion formula was used to compute the new value of the Jaumann integral at time t^{n+1} from its value at t^n [5.5].

The dynamic stiffness apparatus was modeled numerically as shown in Fig. 5.1. The rebound speed was obtained using the *DATABASE_NODOUT ASCII command. To remove the effect of vibration within the ball after the impact, the center node of the

ball was chosen for the rebound speed. Fig.5.2 shows the velocity vs. time data obtained from the *DATABASE_NODOUT ASCII file.

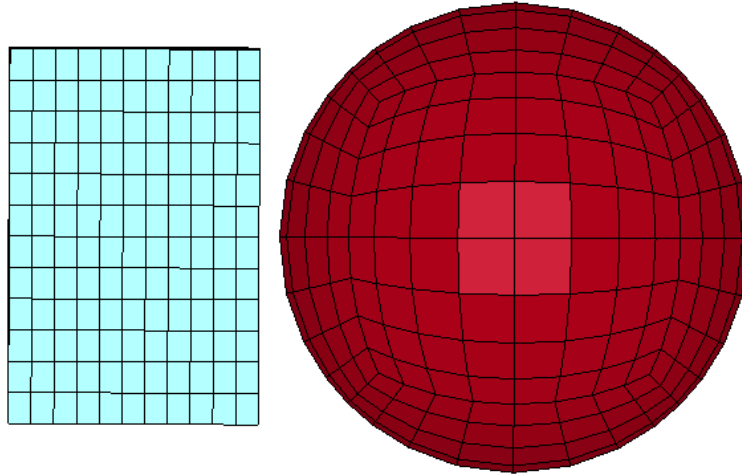


Figure 5.1: Dynamic stiffness apparatus modeled in LS-DYNA.

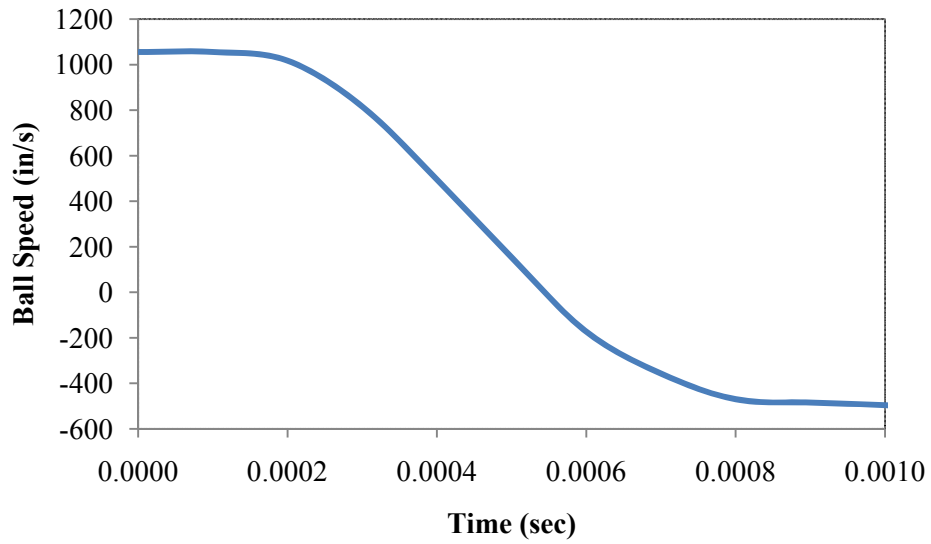


Figure 5.2: A plot of ball speed vs. time.

In Fig. 5.2, the initially positive flat line signifies the speed of the ball before impact whereas the negative flat line represents the speed of the ball after impact with the flat steel plate. The slope between the flat lines corresponds to the compression and expansion phases of the cricket ball. A force was generated when the cricket ball contacted the flat rigid plate. The *DATABASE_RCFORCE ASCII command was used to output the impact force as shown in Fig. 5.3. The ball was impacted at the flat rigid plate at 60mph. Table 5.2 summarizes the viscoelastic properties used for the cricket ball in Fig. 5.1 and 5.3:

Table 5.1: Viscoelastic properties of cricket ball used in following figures

Mass Density (lbs2/in4)	Shear Modulus Short Time(G_0) (psi)	Shear Modulus Long time (G_∞) (psi)	Beta (β)	Elastic Bulk Modulus(K) (psi)
7.96E-05	6300	1667	10500	1.950e4

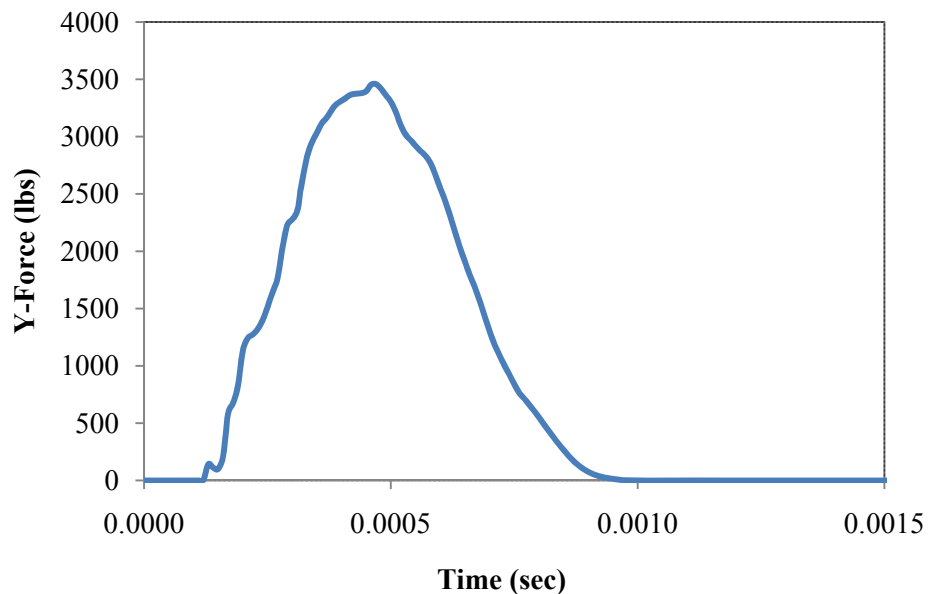


Figure 5.3: Force vs. time plot coarse.

5.2.2 Model Tuning with Experimental Results

A refined cricket model with accurate material properties is necessary to simulate the measured behavior of the cricket ball. Impact simulations are often run with a coarse mesh refinement to reduce solution time.

The standard mesh of the cricket ball consisted of 3584, 8-noded solid elements whereas the fine mesh consisted of 12096, 8-noded solid elements. Fig. 5.4 shows the fine cricket ball mesh. The rigid plate was modeled with dimensions 4 x 1.5 x 2.25 inches using 6336 8-noded solid elements (*ELEMENT_SOLID) and the properties of steel. All nodes on the back side of the rigid plate were constrained to simulate a rigid boundary condition. A contact card (*CONTACT_SURFACE_TO_SURFACE) was used between the cricket ball and steel plate to prevent penetration during impact. The stationary plate was defined as master, and the cricket ball was the slave segment.

The explicit solution was obtained through loops, where the loop time steps were based upon the relative stiffness of the contacting surface. The initial velocity was applied to all the nodes of the cricket ball model, so that every node was given the same initial velocity. The initial velocity of the cricket ball for the finite model was 60mph. The velocity card (*INITIAL VELOCITY) was used to apply the initial velocity to cricket ball. The computational time required to run the standard mesh was 7 minutes, while the fine mesh required approximately 15 minutes. It was observed from the results that the COR and dynamic compression of the fine mesh was 1.8% and 1.0%, respectively higher than the standard mesh. Due to an increased number of elements the force vs. time curve became smoother in the fine mesh as shown in Fig. 5.5.

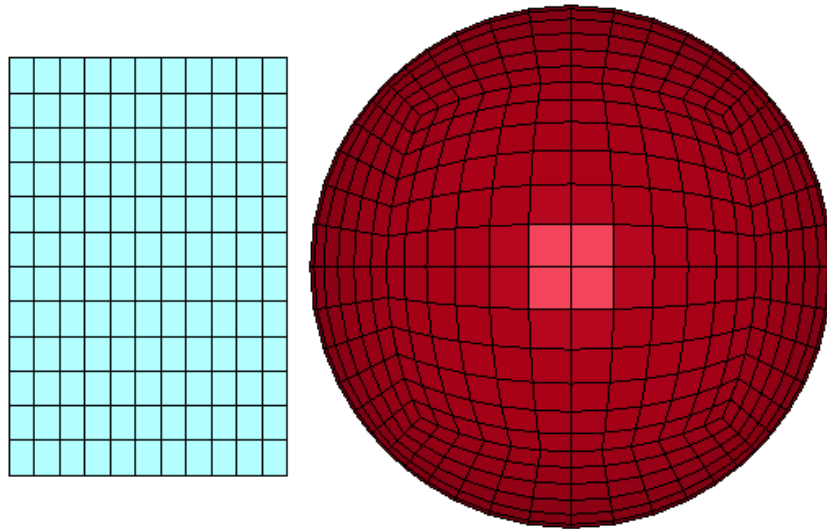


Figure 5.4: Fine mesh of cricket ball dynamic stiffness test (12096 elements).

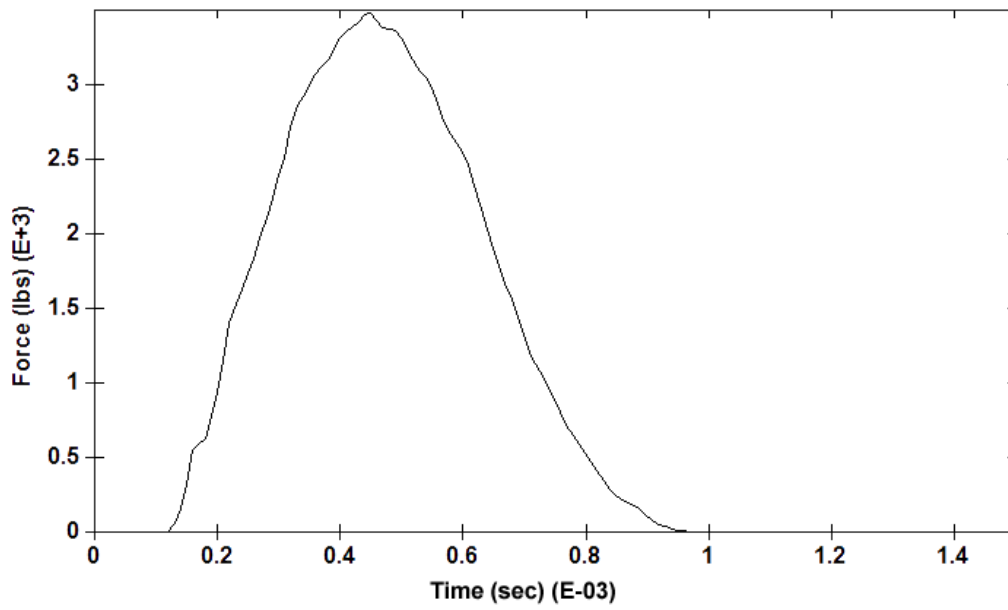


Figure 5.5: Force vs. time curve of fine mesh.

The linear viscoelastic element allows the user to model discrete material properties [5.5]. The viscoelastic properties were adjusted until a good agreement was achieved between the experimental and finite element models. Several parameters have been used in softball and baseball studies in past, as shown in Table 5.2. Fig. 5.6 shows the comparison of finite element and experimental results of cricket ball impacting a load cell at 60mph. Good agreement can be seen between the finite element and experiment.

Table 5.2: Viscoelastic parameter values of Softball and Baseball [5.4]

Model	k (Pa)	G ₀ (pa)	G _∞ (Pa)	β (Hz)
Baseball	27.57x10 ⁹	1.689x10 ⁶	5.86x10 ⁶	850
Softball	27.57x10 ⁹	861.8x10 ³	3.102x10 ⁶	950
Rubber Baseball	19.0x10 ⁶	2.0x10 ⁶	1.0x10 ⁶	1.25x10 ³

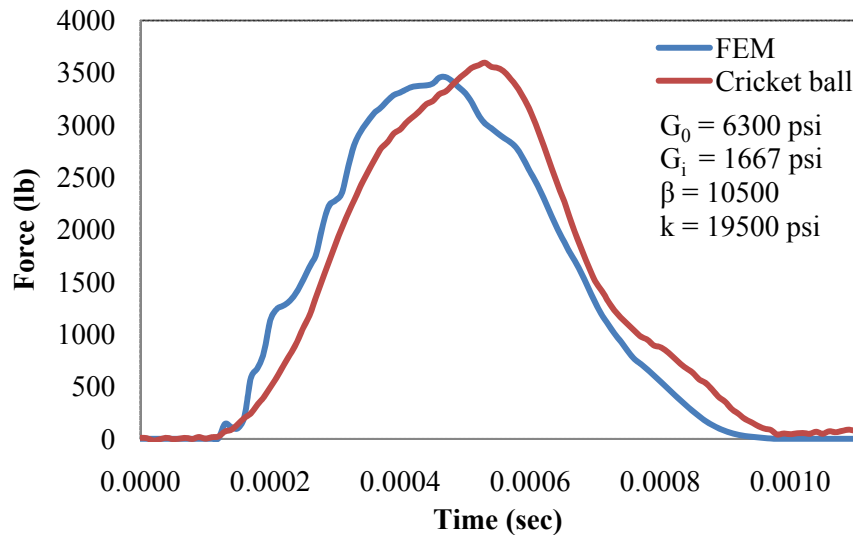


Figure 5.6: Comparison of finite element and experiment of cricket ball impacting a load cell at $v_b = 60\text{mph}$ (26.8 m/s).

While investigating the viscoelastic parameters of the cricket ball, several combinations of G_0 , β , k gave good agreement with the COR and dynamic stiffness of the cricket ball. It was observed that G_0 had greater influence on the dynamic stiffness, where β controlled the COR of the cricket model. Fig. 5.7 represents the effect of β on COR. It was observed that dynamic stiffness decreased with an increase in β , where the COR of the ball was constant. The effect of the long time shear modulus on the COR and dynamic stiffness is shown in Fig. 5.8. It was observed that the COR and dynamic stiffness increased with increasing G_∞ . As shown in Fig. 5.9, the COR decreased whereas the dynamic stiffness increased with an increase in the bulk modulus. The effect of bulk modulus on COR and dynamic stiffness was smaller than the other model parameters considered.

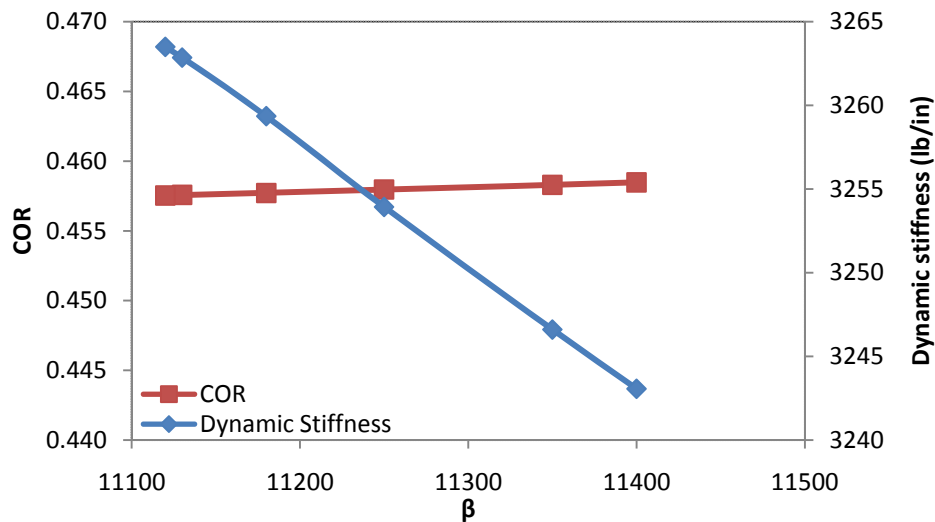


Figure 5.7: β vs. COR and dynamic compression.

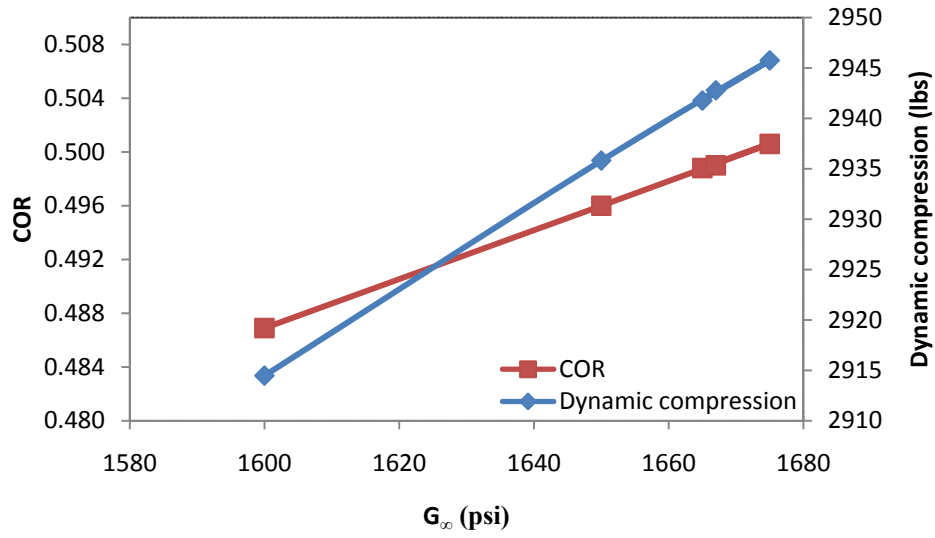


Figure 5.8: Long time shear modulus G_i vs. COR and dynamic compression.

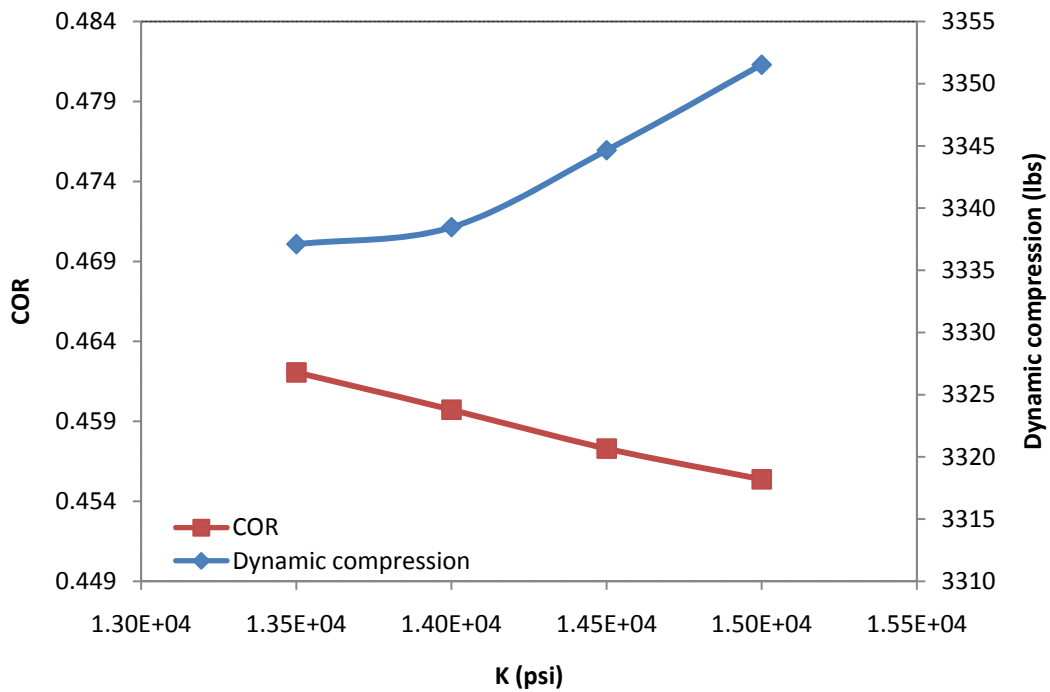


Figure 5.9: Bulk modulus (k) vs. COR and dynamic compression.

5.2.3 Rate Dependence

The finite element model showed good agreement with experimental data over a range of inbound speeds. Fig. 5.10 compares the force-displacement between the finite element model and experiment for ball model B_b. Fig. 5.11 and 5.12 show compare the COR and dynamic stiffness of the finite element model with experimental data as a function of speed. The general trend of COR decreasing with increasing speed was observed for both finite model and experimental data. The experimental COR had steeper curve than finite element model. This occurred for all combinations of material parameters considered. The dynamic stiffness vs. speed of the finite element model and experimental data showed good agreement.

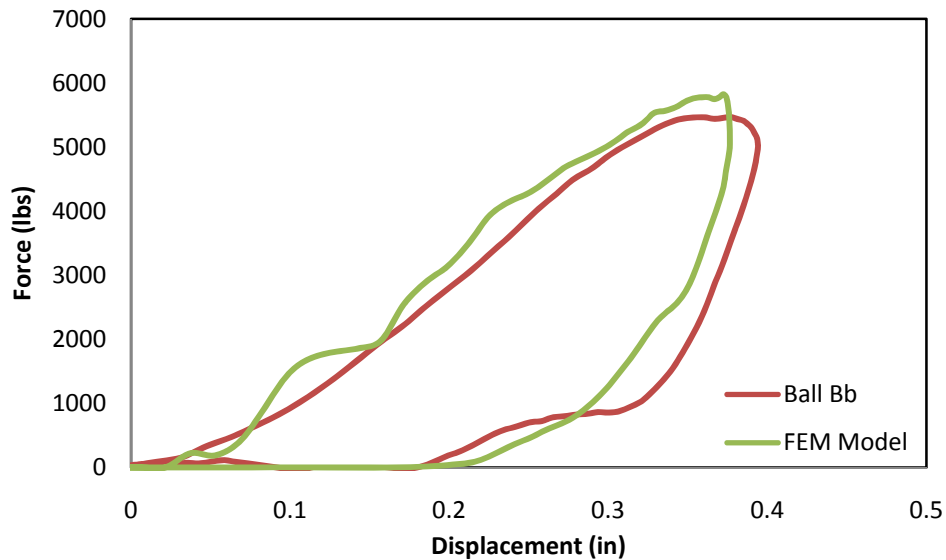


Figure 5.10: Representative force-displacement curve of B_b for experiment and FEM model.

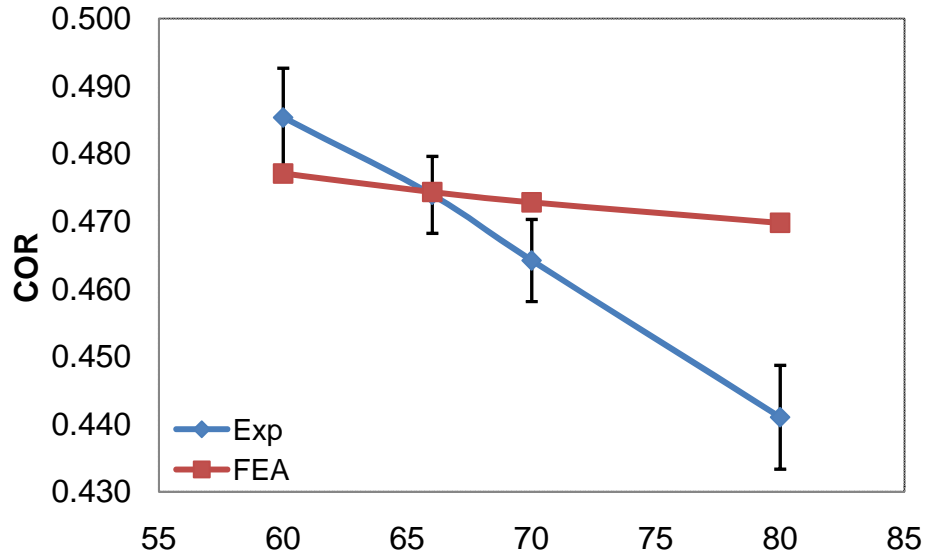


Figure 5.11: Comparison of COR between average of dozen balls and FEA model as a function of incoming speed.

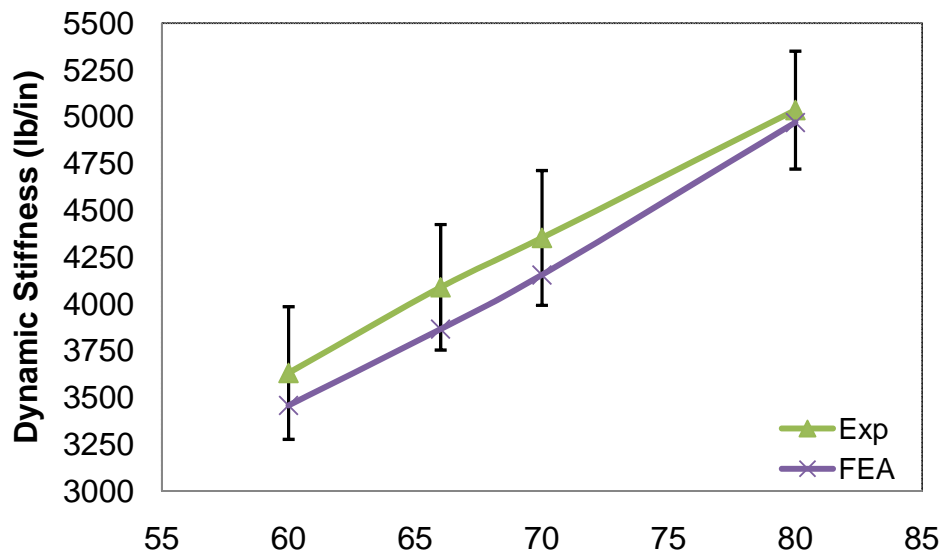


Figure 5.12: Comparison of the dynamic stiffness between the average of 12 balls and FEA model as a function of incoming speed.

5.3 Bat model

5.3.1 Numerical Model

The geometry of each bat model was developed using CATIA Version 5 Revision 17. The geometry of the cricket bat is not simple; it is flat in the blades region and tapers into a cylindrical handle. Two types of coordinate measuring machines (CMM) were used to measure the bat profile (Phytom model and CMM model). The surfaces created from these techniques were irregular, however. Instead, the primary dimensions of the blade and handle were measured and smooth curves were fit to these points to create the surface.

The upper surface of the cricket ball was the slave segment and the lower surface of the cricket bat was the master segment. A surface-to-surface contact algorithm between the bat and ball was used due to the complicated deformation that typically occurs during an explicit dynamic analysis. The mass density of the cricket ball was kept constant at $7.96 \times 10^{-5} \text{ lbs}^2/\text{in}^4$ to provide a ball weight of 5.65 oz. To improve correlation with the measured bat performance β was adjusted as shown in Table 5.3.

Table 5.3: Values of Viscoelastic properties used in the study for Bat-tuned model

Mass Density (lbs^2/in^4)	Shear Modulus Short Time(G_0) (psi)	Shear Modulus Long time (G_i) (psi)	Beta (β)	Elastic Bulk Modulus(K) (psi)
7.96E-05	6300	1667	10500	1.95E+04

5.3.2 Bat Models and Materials

Two cricket bat designs were modeled in this study, a traditional design (M1), and a faceted design (M2) as shown in Fig. 5.13 and 5.14. Wood is an orthotropic material, thus its properties in the longitudinal, radial and transverse directions are different.

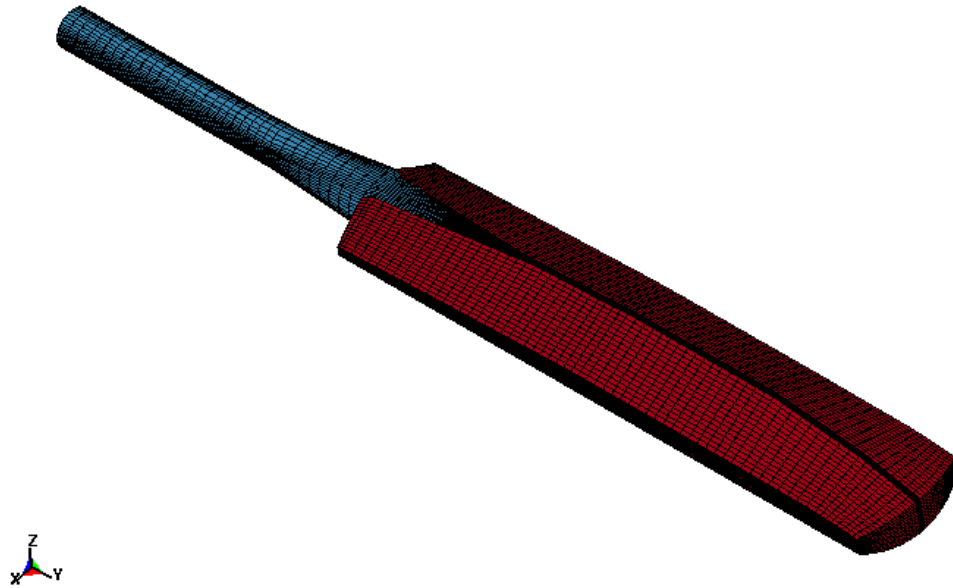


Figure 5.13: Traditional design (M1) Bat model.

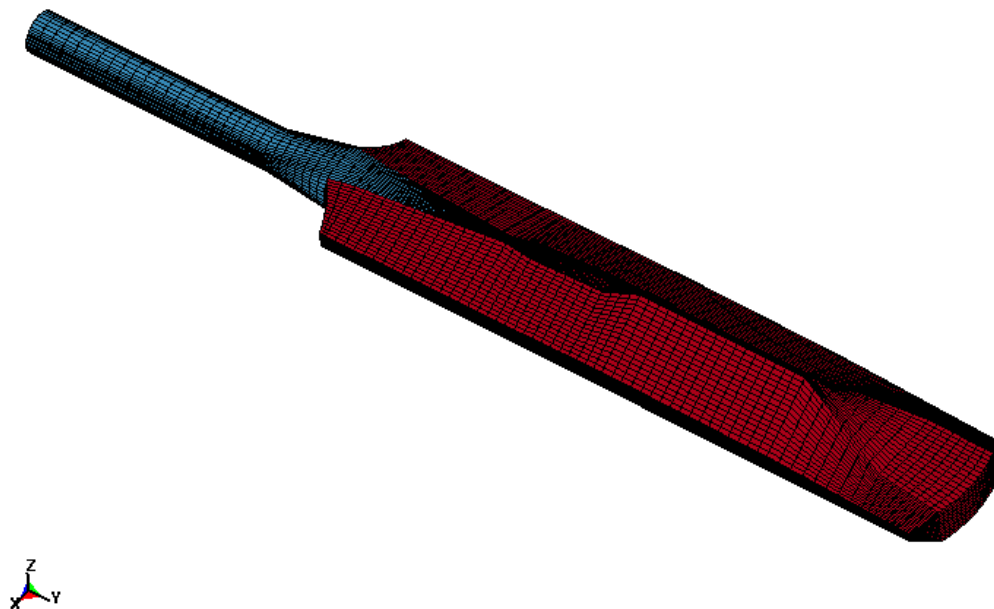


Figure 5.14: Faceted design (M2) bat model.

Wood is a natural material and its density varies from species to species. The density of willow and cane varies from $4.24 \times 10^{-4} \text{ lbs}^2/\text{in}^4$ to $7.018 \times 10^{-5} \text{ lbs}^2/\text{in}^4$ [5.8], and $6.74 \times 10^{-5} \text{ lbs}^2/\text{in}^4 - 4.29 \times 10^{-5} \text{ lbs}^2/\text{in}^4$ [5.9], respectively. The density of the willow and cane were tailored to match the measured weight and mass moment of inertia (MOI) of the bat. Willow and cane elastic properties are summarized in Table 5.5. The elastic properties of the cane handle have a small effect on bat performance. The transverse properties of the handle are even less important. For this reason, and since the orthotropic properties of cane are not known, it was assumed to be isotropic.

Table 5.4: Values of Viscoelastic properties used in the study for Bat-tuned model

Mass Density (lbs^2/in^4)	Shear Modulus Short Time (G_0) (psi)	Shear Modulus Long time (G_∞) (psi)	Beta (β)	Elastic Bulk Modulus (K) (psi)
7.89E-05	4750	1667	10500	1.95E+04

Table 5.5: Elastic Properties of Cricket Bat (Coordinate system as in Fig. 5.14 and 5.15)

	Young's Modulus (Msi)			Mass Density (lbs ² /in ⁴)	Shear Modulus (Msi)			Poisson's ratio		
	E _x	E _y	E _z	ρ ₀	G _{xy}	G _{yz}	G _{zx}	ν _{yx}	ν _{zx}	ν _{zy}
Willow	0.479	0.0319	0.255	4.14x10 ⁻⁵	0.0479	0.00479	0.0479	0.015	0.16	0.6
Cane	0.318	0.318	0.318	4.66x10 ⁻⁵	-	-	-	0.3	0.3	0.3

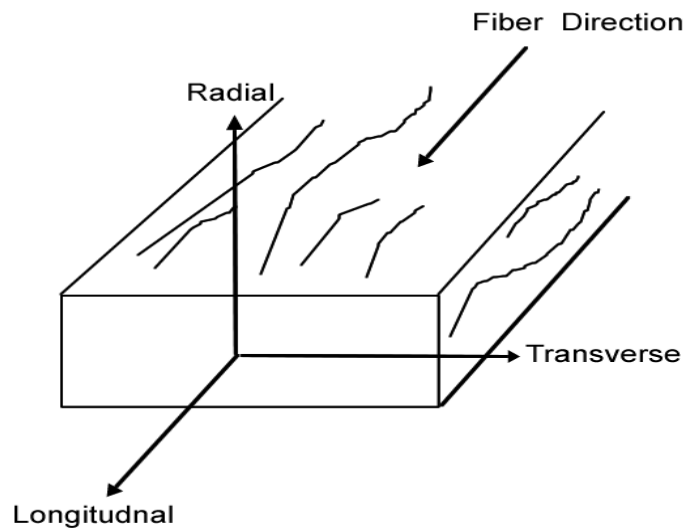


Figure 5.15: Principal axis of wood.

The composite skin was modeled using the properties of carbon epoxy AS4/3501-6 with a [0/90]_s layup of thickness 0.02 inches. The laminated properties of the composite skin are presented in Table 5.6.

Table 5.6: Laminated [0/90]_s Properties of Composite Skin

	Young's Modulus (Msi)			Mass Density (lbs ² /in ⁴)	Shear Modulus (Msi)			Poisson's ratio		
	E _x	E _y	E _z	ρ ₀	G _{xy}	G _{yz}	G _{zx}	ν _{yx}	ν _{zx}	ν _{zy}
Composite	11.1	11.1	1.14	1.55x10 ⁻⁴	1.04	0.912	0.912	0.037	0.0158	0.26

5.3.3 Modeling the Bat-Ball Impact

The *BOUNDARY_SPC_NODE_ID card was used to constrain the nodes at the pivot point. A termination time of 0.003s was used to allow for initial ball motion, the bat-ball impact period and the rebound ball motion.

A comparison between the experiment and FEA length and mass properties is given in Table 5.7 and 5.8. The mass properties of the bat with and without the composite skin are compared in Table 5.8.

Table 5.7: Comparison of measured and modeled M1 bat properties

	Length (in)	Weight (oz)	MOI (oz-in ²)
Experimental	33.54	37.68	9799
FE Model	33.54	37.68	9779
% Difference	0.000	0.000	0.199

Table 5.8: Comparison of measured and modeled M2 bat properties

	Length (in)	Weight (oz)	MOI (oz-in ²)
Experimental	34.92	39.54	11778
FE Model	34.92	41.9	11711
% Difference	0.000	-5.6	0.579

5.4 Experimental Comparison

The elastic properties of the wood can vary within the same species. A study was conducted to consider the effect of elastic properties in each direction independently on bat performance. When the radial modulus was doubled, the BBS increased by 1%. While the BBS increased by 2% when the tangential modulus was doubled. It was also observed that there was 10% increase in BBS when the longitudinal modulus was doubled.

The performance of the M1 model is shown in Figure 5.16. The model shows good agreement with the experiment. Model M2 is compared with experiment over an extended impact location range in Fig. 5.17. Note the relatively small region which produces a maximum BBS.

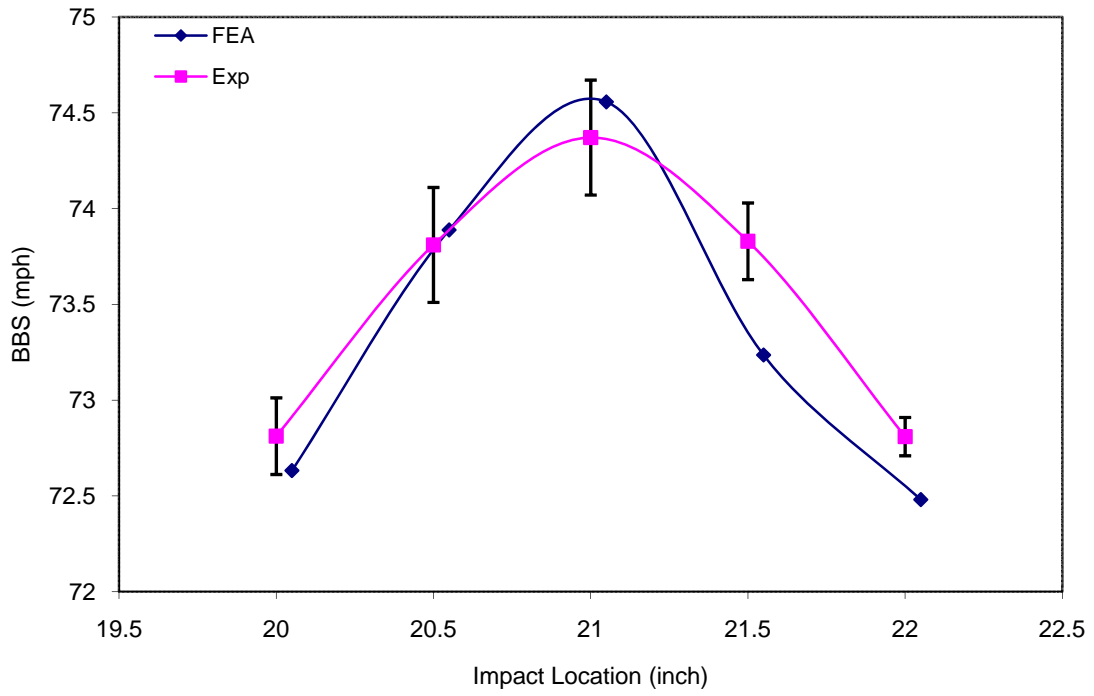


Figure 5.16: Experimental validation of the M1 model at different impact locations.

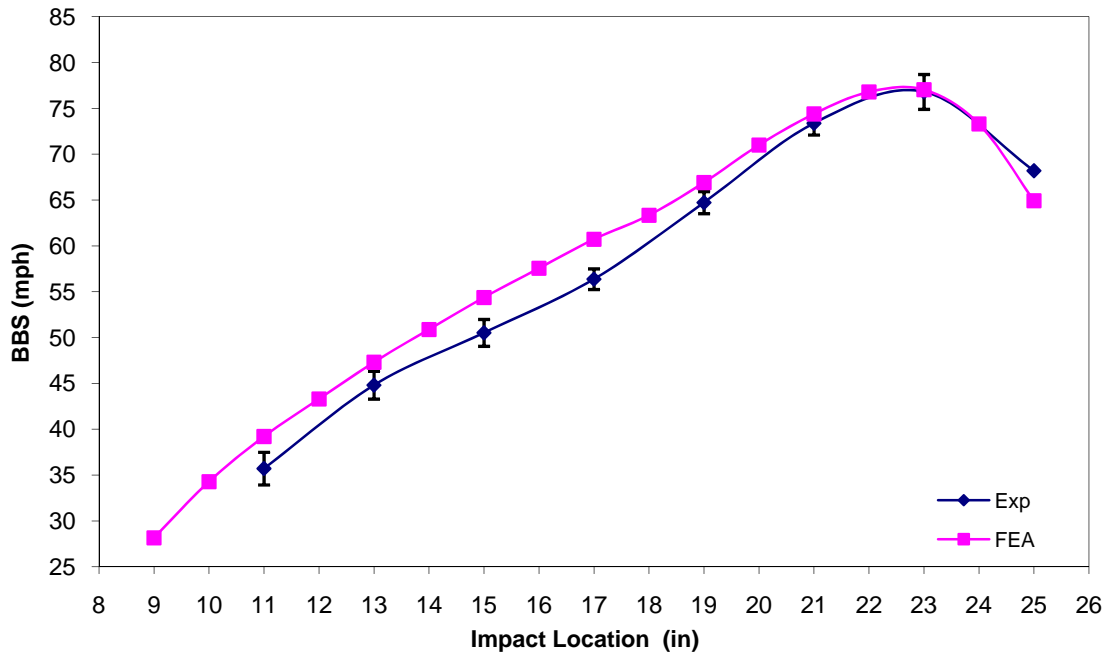


Figure 5.17: Representative performance curves for bat and model.

5.4.1 Weight study

Results from the previous studies show that adding weight at a sufficient distant from the impact location will not affect the performance of the bat. A study was conducted to check the behavior of the bat model when weight was added at different positions in the model.

The study involved adding 2 oz of weight at different locations along the cricket bat. The ball was impacted at the peak BBS position of the bat model. Fig. 5.18 shows the change in MOI for the added weight at each position of the bat model. It was observed that the MOI changed by at most 12% from the added weight.

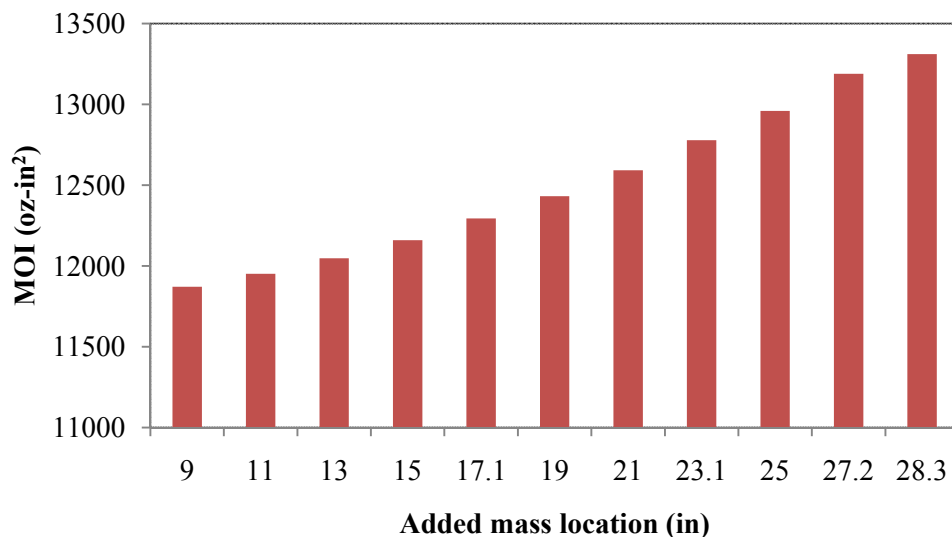


Figure 5.18: MOI of the bat model when weight was added at different locations.

The BBS is shown as a function of weight location in Fig. 5.19. The BBS varied by 1% with the different weight locations. The BBCOR should be less sensitive to MOI and is included in Fig 5.19, where it changed 1% with weight location. Following Eq. 4.8

the BBCOR is independent of inbound speed and the mass of the bat, so the BBCOR should be consistent with the change in MOI by adding mass at different locations.

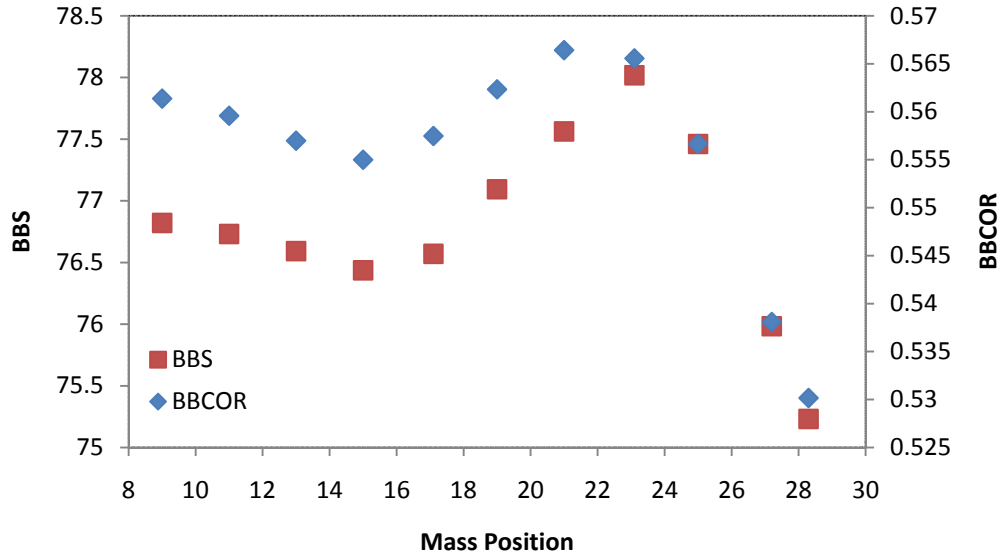


Figure 5.19: BBCOR as a function of weight location from the pivot.

5.4.2 Composite Skin

The mass properties of two bats with and without a skin are compared in Table 5.9. The performance of a bat was compared with and without a composite skin, as shown in Fig. 5.20. The effect of the 0.02 inch thick composite skin was considered in the numeric model using the properties of Table 5.8. The results are included in Fig. 5.20 and 5.21, where the skin increased the BBS by 2.2%. The FEA model had a different geometry than was tested experimentally. Therefore, the MOI of the FEA model was reduced to match the experimentally tested bat. A composite skin weighting 1.6 oz was considered in the numeric study; taken as average of the two composite bats tested.

Table 5.9: Properties of Cricket bat and FEA used in the performance comparison.

	Material	Length (in)	Weight (oz)	MOI (oz in ²)
Experiment	Willow, Cane	33.8	36.8	10462
	Willow, Cane, Composite	33.8	38.3	10792
FE Model	Willow, Cane	34.3	41.9	10462
	Willow, Cane, Composite	34.3	39.5	11021

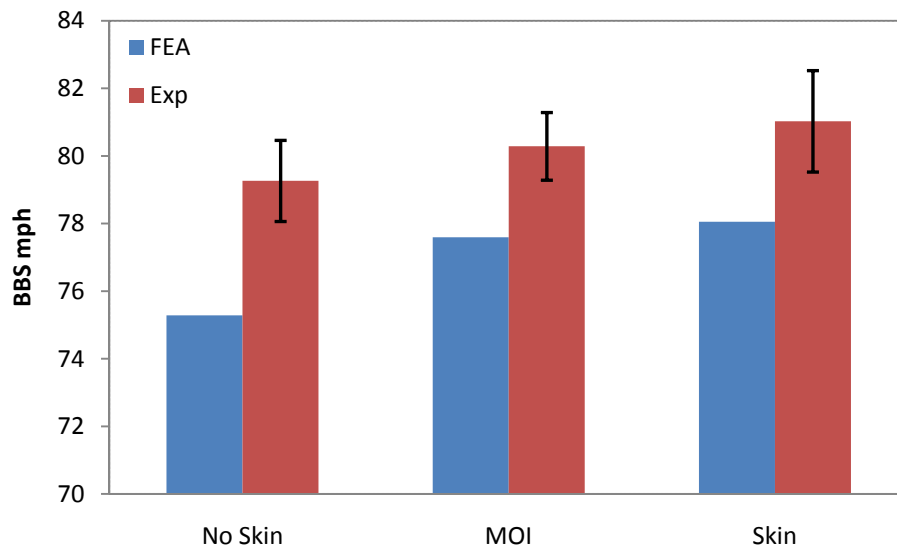


Figure 5.20: Comparison of finite element model and cricket bat with and without composite skin.

5.5 Summary:

A finite element model has been used to describe the performance of a two cricket bat models. The models were developed to accurately describe the geometry and weight of the cricket bats tested experimentally. The models showed good agreement with the experimental data for bat and ball performance. Mass distribution and composite

reinforcement were shown to have a measurable effect on bat performance. In comparison with hollow baseball and softball bats, however, the effect was relatively small.

References:

- [5.1] Nicolls, R.L., Miller, K., and Elliott, B.C. "Modeling Deformation Behavior of the Baseball" *Journal of Applied Biomechanics*. pp: 18-30. 2005.
- [5.2] Mustone, T.J., Sherwood, J.A "Using Ls-Dyna to Characterize the Performance of Baseball Bats" 5th International Ls-Dyna Users Conference, South-field, MI. Livermore, CA: Livermore Software Technology Corp. pp: 21-22, Sept. 1998.
- [5.3] Cook, D.R. "Concepts And Applications Of Finite Element Analysis" Fourth Edition.
- [5.4] Smith, L.V, Shenoy, M.M., Axtell, J.T. "Performance assessment of wood, metal and composite baseball bats". ASME IMECE, 2000
- [5.5] LS-DYNA Keyword Users Manual. Liversome Software Technology Corporation. August 2007. Version 971
- [5.6] Biesen, E. D., "Prediction of plastic Deformation in Aluminum Softball Bats Using Finite Element Analysis" Washington State University. August 2006.
- [5.7] Penrose. J. M. T., Hose, D. R. "Finite Element Impact Analysis of a Flexible Cricket Bat for Design Optimization" *The Engineering of Sports*. 1998
- [5.8] Khanduri, A.K., Shukla, N.K. "Physical and Mechanical Properties of Salix Alba- An Assessment" *J. Timb. Dev. Assoc. (India)* Vol. XLIV. Nov 4, October 1998
- [5.9] Barizan, R. S. R., Aswad, R.M. "Cane Properties of Cultivated Rotan Manau under Second Growth Forests: Relations Between Maturity and Strength" *Highlights of FRIM's IRPA projects*. Pp. 186-191. 2005.
- [5.10] Cook, R.D. "Finite Element Modeling for Stess Analysis" John Wiley and Sons, Inc.

CHAPTER 6

-SUMMARY-

6.1 Review

The study measured and compared the performance of different models of cricket balls and bats. The following summarizes the major findings of this work.

6.2 Ball Testing

A high-speed canon was used to measure the dynamic properties of cricket balls by impacting a rigid wall at 60 – 80mph. The COR of all the cricket balls decreased with increasing impact speed. Seam impacts had a higher COR and dynamic stiffness than a face impacts. A gradual increase in displacement and force with impact speed was observed in both seam and face impacts. The relationship between the peak force and impact speed was non-linear. The ball model with a rubber core had lower COR and variation than the ball model which contained a cork core.

6.3 Bat Testing

A test apparatus was developed to measure bat properties at impact speeds representative of the play conditions. The test method involved firing the cricket balls at various positions on a stationary cricket bat. A bat performance measure was derived in terms of an ideal batted-ball speed based on play conditions. The swing speed of the cricket bat was found from the flight of the cricket ball. The MOI of the cricket bat had a measureable effect on bat performance. Knock-in and oiling had a smaller effect than weight or MOI on performance.

Wood species had a relatively small effect where the performance of English willow bats was on average 0.84% higher than Kashmir willow bats. The contribution of a reinforcing composite skin to the back surface of the bat was also relatively small (1.4%), although larger than the effect of knock-in or willow species. It should be noted, however, that one half of this advantage was due to the weight of the composite. While the different treatments and designs had a measurable effect on performance, they were much smaller than the 10% difference observed between solid wood and hollow baseball and softball bats.

6.4 Numeric model

A dynamic finite element model was employed to simulate the bat-ball impact. The ball was modeled as a linear viscoelastic material which provided the mechanism of energy loss during impact. The ball model was tuned by adjusting its material properties to match its measurable response. The model showed good agreement with the experimental data for bat and ball performance. Mass distribution and composite reinforcement were shown to have a measurable effect on bat performance. In comparison with hollow baseball and softball bats, however, the effect was relatively small.

6.5 Future work

The work performed here was successful to answer many questions related to the performance of cricket bats. However, there are many issues deserving for further investigation.

It was shown that cricket balls had a significant effect on the performance of cricket bats. For changes to be implemented, additional data of COR and dynamic stiffness at several speeds is needed. More investigation is needed on seam and face impacts.

Another area of research is numeric modeling. Refinement of the mesh density need to be further investigated. Another area that needs to be addressed is the orthotropic properties of willow.

APPENDIX ONE

Detailed information used for cricket bat model with composite skin

```

*KEYWORD
*TITLE
$# title
LS-DYNA keyword deck by LS-PRE
*CONTROL_TERMINATION
$# endtim      endcyc      dtmin      endeng      endmas
   0.002000
*DATABASE_ELOUT
$#      dt      binary
   1.0000X10-4      1
*DATABASE_NODOUT
$#      dt      binary
   1.0000X10-5      1
*DATABASE_RCFORC
$#      dt      binary
   1.0000X10-5      1
*DATABASE_BINARY_D3PLOT
$#      dt      lcdt      beam      npltc
   1.0000X10-4
$#  ioopt
      0
*DATABASE_HISTORY_NODE
$#      id1      id2      id3      id4      id5      id6      id7
id8
      57685      6059      6072      57604
*BOUNDARY_SPC_NODE
$#      nid      cid      dofz      dofry
dofrz
      14151      0      0      1      1
      14268      0      0      1      1
      14385      0      0      1      1
      14502      0      0      1      1
      14619      0      0      1      1
      14736      0      0      1      1
      14853      0      0      1      1
      14970      0      0      1      1
      15087      0      0      1      1
      15204      0      0      1      1
      15321      0      0      1      1
      15438      0      0      1      1
      15555      0      0      1      1
      15672      0      0      1      1
      15789      0      0      1      1
      15906      0      0      1      1
      16023      0      0      1      1
*CONTACT_SURFACE_TO_SURFACE_ID
$#      cid
title
      1
$#      ssid      msid      sstyp      mstyp      sboxid      mboxid      spr
mpr
      2      1

```

```

$#      fs      fd      dc      vc      vdc      penchk      bt
dt
      0.000      0.000      0.000      0.000      0.000      0
0.0001.0000E+20
$#      sfs      sfm      sst      mst      sfst      sfmt      fsf
vsf
      1.000000      1.000000      0.000      0.000      1.000000      1.000000      1.000000
1.000000
*SET_SEGMENT_TITLE
Ball
$#      sid      da1      da2      da3      da4
      2
$#      n1      n2      n3      n4      a1      a2      a3
a4
      59386      59395      59396      59387
      59395      59404      59405      59396
      59404      59413      59414      59405
      59413      59422      59423      59414
      59422      60088      60089      59423
      60088      60097      60098      60089
      '      '      '      '
*SET_SEGMENT_TITLE
Willow
$#      sid      da1      da2      da3      da4
      1
$#      n1      n2      n3      n4      a1      a2      a3
a4
      8087      8100      8334      8321
      8321      8334      8568      8555
      8555      8568      8802      8789
      '      '      '      '
*PART
$# title
Willow
$#      pid      secid      mid      eosid      hgid      grav      adpopt
tmid
      1      1      1
*SECTION_SOLID_TITLE
Willow
$#      secid      elform      aet
      1      1
*MAT_ORTHOTROPIC_ELASTIC_TITLE
Willow
$#      mid      ro      ea      eb      ec      prba      prca
prcb
      1      4.1450X10-5      4.7860E+5      31910.000      2.5520E+5      0.015000
0.160000      0.600000
$#      gab      gbc      gca      aopt      g      sigf
      47860.000      4786.0000      47860.000      2.000000
$#      xp      yp      zp      a1      a2      a3
      0.000      0.000      0.000      0.000      1.000000
$#      v1      v2      v3      d1      d2      d3      beta
ref
      0.000      0.000      0.000      1.000000      1.000000
*PART
$# title
Handle Cane

```

```

$#   pid   secid   mid   eosid   hgid   grav   adpopt
tmid
      2     2     2
*SECTION_SOLID_TITLE
Handle Cane
$#   secid   elform   aet
      2     1
*MAT_ELASTIC_TITLE
Handle Cane
$#   mid     ro       e       pr       da       db   not used
      2 4.6790X10-5 1.5910E+5 0.300000
*PART
$# title
Ball
$#   pid   secid   mid   eosid   hgid   grav   adpopt
tmid
      3     3     3
*SECTION_SOLID_TITLE
Ball
$#   secid   elform   aet
      3     1
*MAT_VISCOELASTIC_TITLE
Ball
$#   mid     ro       bulk     g0       gi       beta
      3 7.9600X10-5 19500.000 4750.0000 1667.0000 10500.000
*PART
$# title
Composite Skin
$#   pid   secid   mid   eosid   hgid   grav   adpopt
tmid
      4     4     4
*SECTION_SHELL_TITLE
Composite Skin
$#   secid   elform   shrf     nip     propt   qr/irid   icomp
setyp
      4     2 1.000000     2     1     0     0
1
$#   t1     t2     t3     t4     nloc     marea     idof
edgset
 0.025000 0.025000 0.025000 0.025000
*MAT_ORTHOTROPIC_ELASTIC_TITLE
Composite skin
$#   mid     ro       ea       eb       ec       prba     prca
prcb
      4 5.5400X10-5 1.1090E+7 1.1090E+7 1.1430E+6 0.037000
0.015800 0.260000
$#   gab     gbc     gca     aopt     g     sigf
1.0400E+6 9.1190E+5 9.1190E+5 2.000000
$#   xp     yp     zp     a1     a2     a3
0.000     0.000     0.000     0.000     1.000000
$#   v1     v2     v3     d1     d2     d3     beta
ref
0.000     0.000     0.000     1.000000 1.000000
*INITIAL_VELOCITY
$#   nsid     nsidex   boxid   irigid
3
$#   vx     vy     vz     vxr     vyr     vzr

```

```

0.000      0.000 1056.0000
*SET_NODE_LIST_TITLE
Willow
$#      sid      da1      da2      da3      da4
      1
$#      nid1      nid2      nid3      nid4      nid5      nid6      nid7
nid8
      1      2      3      4      5      6      7
8
      9      10      11      12      13      14      15
16
      17      18      19      20      21      22      23
24
      25      26      27      28      29      30      31
      37839      37840      37841      37842      37843      37844      37845
*SET_NODE_LIST_TITLE
Handle Cane
$#      sid      da1      da2      da3      da4
      2
$#      nid1      nid2      nid3      nid4      nid5      nid6      nid7
nid8
      11935      11936      11937      11938      11939      11940      11941
11942
      11943      11944      11945      11946      11947      11948      11949
*SET_NODE_LIST_TITLE
Ball
$#      sid      da1      da2      da3      da4
      3
$#      nid1      nid2      nid3      nid4      nid5      nid6      nid7
nid8
      57240      57241      57242      57243      57244      57245      57246
57247
      57248      57249      57250      57251      57252      57253      57254
*ELEMENT_SOLID
$#      eid      pid      n1      n2      n3      n4      n5      n6
n7      n8
      1      1      1      235      248      14      2      236
249      15
      2      1      2      236      249      15      3      237
*ELEMENT_SHELL
$#      eid      pid      n1      n2      n3      n4      n5      n6
n7      n8
      48898      4      55484      55367      55354      55471
      48899      4      55601      55484      55471      55588
*NODE
$#      nid      x      y      z      tc
rc
      1      11.30500031      7.19999933      -12.39999962
      2      11.30500031      7.19999933      -12.22083378
*END

```


APPENDIX TWO

Detailed information used for cricket bat model in weight study

```

*KEYWORD
*TITLE
$# title
LS-DYNA keyword deck by LS-PRE
*CONTROL_TERMINATION
$#  endtim      endcyc      dtmin      endeng      endmas
    0.002500
*DATABASE_ELOUT
$#      dt      binary
    1.0000X10-4      1
*DATABASE_NODOUT
$#      dt      binary
    1.0000X10-5      1
*DATABASE_RCFORC
$#      dt      binary
    1.0000X10-5      1
*DATABASE_BINARY_D3PLOT
$#      dt      lcdt      beam      npltc
    1.0000X10-4
$#  ioopt
    0
*DATABASE_HISTORY_NODE
$#      id1      id2      id3      id4      id5      id6      id7
id8
    57685      6059      6072      57604
*BOUNDARY_SPC_NODE
$#      nid      cid      dofz      dofry
dofrz
    14151      0      0      1      1
    14268      0      0      1      1
    14385      0      0      1      1
*CONTACT_SURFACE_TO_SURFACE_ID
$#      cid
title
    1
$#      ssid      msid      sstyp      mstyp      sboxid      mboxid      spr
mpr
    2      1
$#      fs      fd      dc      vc      vdc      penchk      bt
dt
    0.000      0.000      0.000      0.000      0.000      0
0.0001.0000E+20
$#      sfs      sfm      sst      mst      sfst      sfmt      fsf
vsf
    1.000000      1.000000      0.000      0.000      1.000000      1.000000      1.000000
1.000000
*SET_SEGMENT_TITLE
Ball
$#      sid      da1      da2      da3      da4

```

```

      2
$#    n1      n2      n3      n4      a1      a2      a3
a4
      59386      59395      59396      59387

```

*SET_SEGMENT_TITLE

Willow

```

$#    sid      da1      da2      da3      da4
      1
$#    n1      n2      n3      n4      a1      a2      a3
a4
      8087      8100      8334      8321
      8321      8334      8568      8555

```

*PART

\$# title

Willow

```

$#    pid      secid      mid      eosid      hgid      grav      adpopt
tmid
      1      1      1

```

*SECTION_SOLID_TITLE

Willow

```

$#    secid      elform      aet
      1      1

```

*MAT_ORTHOTROPIC_ELASTIC_TITLE

Willow

```

$#    mid      ro      ea      eb      ec      prba      prca
prcb
      1 4.1450X10-5 4.7860E+5 31910.000 2.5520E+5 0.015000
0.160000 0.600000
$#    gab      gbc      gca      aopt      g      sigf
      47860.000 4786.0000 47860.000 2.000000
$#    xp      yp      zp      a1      a2      a3
      0.000      0.000      0.000      0.000 1.000000
$#    v1      v2      v3      d1      d2      d3      beta
ref
      0.000      0.000      0.000 1.000000 1.000000

```

*PART

\$# title

Handle Cane

```

$#    pid      secid      mid      eosid      hgid      grav      adpopt
tmid
      2      2      2

```

*SECTION_SOLID_TITLE

Handle Cane

```

$#    secid      elform      aet
      2      1

```

*MAT_ELASTIC_TITLE

Handle Cane

```

$#    mid      ro      e      pr      da      db      not used
      2 4.6790X10-5 1.5910E+5 0.300000

```

*PART

\$# title

Ball

```

$#    pid      secid      mid      eosid      hgid      grav      adpopt
tmid
      3      3      3

```

```

*SECTION_SOLID_TITLE
Ball
$#   secid   elform   aet
      3       1
*MAT_VISCOELASTIC_TITLE
Ball
$#   mid     ro       bulk     g0       gi       beta
      3 7.9600X10-5 19500.000 4750.0000 1667.0000 10500.000
*INITIAL_VELOCITY
$#   nsid   nsidex   boxid   irigid
      3
$#   vx     vy       vz       vxr     vyr     vzr
      0.000 0.000 1056.0000
*SET_NODE_LIST_TITLE
Willow
$#   sid     da1     da2     da3     da4
      1
$#   nid1   nid2     nid3     nid4     nid5     nid6     nid7
nid8
      1       2       3       4       5       6       7
8
      9       10      11      12      13      14      15
*SET_NODE_LIST_TITLE
Ball
$#   sid     da1     da2     da3     da4
      3
$#   nid1   nid2     nid3     nid4     nid5     nid6     nid7
nid8
      57240  57241  57242  57243  57244  57245  57246
57247
*ELEMENT_SOLID
$#   eid     pid     n1     n2     n3     n4     n5     n6
n7     n8
      1       1       1     235   248   14     2     236
249    15
      2       1       2     236   249   15     3     237
*ELEMENT_MASS
$#   eid     nid     mass     pid
      1     47912 3.2379999e-004 1
*NODE
$#   nid     x       y       z       tc
rc
      1     11.30500031 7.19999933 -12.39999962
      2     11.30500031 7.19999933 -12.22083378
      3     11.30500031 7.19999933 -12.04166603
      4     11.30500031 7.19999933 -11.86250019

```

APPENDIX THREE

Detailed information used for cricket ball model

```
*KEYWORD
*TITLE
$# title
LS-DYNA keyword deck by LS-PRE
*CONTROL_TERMINATION
$# endtim   endcyc   dtmin   endeng   endmas
   0.003000
*DATABASE_ELOUT
$#   dt   binary
   1.0000X10-4   1
*DATABASE_NODOUT
$#   dt   binary
   1.0000X10-5   1
*DATABASE_RCFORC
$#   dt   binary
   1.0000X10-5   1
*DATABASE_BINARY_D3PLOT
$#   dt   lcdt   beam   npltc
   1.0000X10-5
$#   ioopt
   0
*DATABASE_HISTORY_NODE
$#   id1   id2   id3   id4   id5   id6   id7
id8
   8321
*BOUNDARY_SPC_NODE
$#   nid   cid   dofz   dofry
dofrz
   144   0   1   1   1
   145   0   1   1   1
*CONTACT_SURFACE_TO_SURFACE_ID
$#   cid
title
   1
$#   ssid   msid   sstyp   mstyp   sboxid   mboxid   spr
mpr
   1   2
$#   fs   fd   dc   vc   vdc   penchk   bt
dt
   0.000   0.000   0.000   0.000   0.000   0
0.0001.0000E+20
$#   sfs   sfm   sst   mst   sfst   sfmt   fsf
vsf
   1.000000   1.000000   0.000   0.000   1.000000   1.000000   1.000000
1.000000
*SET_SEGMENT_TITLE
Ball
$#   sid   da1   da2   da3   da4
   1
```

```

$#      n1      n2      n3      n4      a1      a2      a3
a4
      10823    10832    10833    10824
      10825    10834    10835    10826
*SET_SEGMENT_TITLE
Plate
$#      sid      da1      da2      da3      da4
      2
$#      n1      n2      n3      n4      a1      a2      a3
a4
      636      637      481      480
      635      636      480      479
      634      635      479      478
*PART
$# title
Ball
$#      pid      secid      mid      eosid      hgid      grav      adpopt
tmid
      1      1      1
*SECTION_SOLID_TITLE
Ball
$#      secid      elform      aet
      1      1
*MAT_VISCOELASTIC_TITLE
Ball
$#      mid      ro      bulk      g0      gi      beta
      1 7.9600X10-5 19500.000 6300.0000 1667.0000 10500.000
*PART
$# title
Plate
$#      pid      secid      mid      eosid      hgid      grav      adpopt
tmid
      2      2      2
*SECTION_SOLID_TITLE
Plate
$#      secid      elform      aet
      2      1
*MAT_ELASTIC_TITLE
Plate
$#      mid      ro      e      pr      da      db      not used
      2 7.7000X10-4 2.9000E+7 0.300000
*INITIAL_VELOCITY
$#      nsid      nsidex      boxid      irigid
      1
$#      vx      vy      vz      vxr      vyr      vzr
      0.000 1056.0000
*SET_NODE_LIST_TITLE
Ball
$#      sid      da1      da2      da3      da4
      1
$#      nid1      nid2      nid3      nid4      nid5      nid6      nid7
nid8
      9375      7957      7958      7959      7960      7961      7962
7963
      7964      7965      7966      7967      7968      7969      7970
*SET_NODE_LIST_TITLE
Plate

```

```

$#      sid      da1      da2      da3      da4
      2
$#      nid1      nid2      nid3      nid4      nid5      nid6      nid7
nid8
      1      2      3      4      5      6      7
8
      9      10      11      12      13      14      15
*ELEMENT_SOLID
$#      eid      pid      n1      n2      n3      n4      n5      n6
n7      n8
      1      2      1      157      170      14      2      158
171      15
      2      2      2      158      171      15      3      159
*NODE
$#      nid      x      y      z      tc
rc
      1
      2      0.000      0.000      0.18750000
      3      0.000      0.000      0.37500000
      4      0.000      0.000      0.56250000
      5      0.000      0.000      0.75000000
      6      0.000      0.000      0.93750012
      7      0.000      0.000      1.12500012
      8      0.000      0.000      1.31250024
      9      0.000      0.000      1.50000024
     10      0.000      0.000      1.68750024
     11      0.000      0.000      1.87500012
     12      0.000      0.000      2.06250000
     13      0.000      0.000      2.25000000
     14 -6.9099206e-009      0.13636364 -8.1634539e-009
     15 -6.1238374e-009      0.13636364      0.18749999
     16 -5.3377538e-009      0.13636364      0.37499997
     17 -4.5516706e-009      0.13636366      0.56250000
*END

```